Design of Interactive Maps for Ocean Dynamics Data

by

Mohamad Mirhi

B.E., American University of Beirut (2011)
S.M., Massachusetts Institute of Technology (2013)

Submitted to the Department of Mechanical Engineering in partial fulfillment of the requirements for the degree of

Mechanical Engineer

at the

MASSACHUSETTS INSTITUTE OF TECHNOLOGY

February 2019

Signature redacted

Author ....
Department of Mechanical Engineering
19 September 2018

Signature redacted

Certified by...... ....
Pierre Lermusiaux
Professor, Associate Department Head for Operations
Thesis Supervisor

Signature redacted

Accepted by ....
Nicolas Hadjiconstantinou
Chairman, Committee on Graduate Students

Design of Interactive Maps for Ocean Dynamics Data

by

Mohamad Mirhi

Submitted to the Department of Mechanical Engineering
on 19 September 2018, in partial fulfillment of the
requirements for the degree of
Mechanical Engineer

Abstract

Comprehensive spatiotemporal modeling and forecasting systems for ocean dynamics necessitate robust and efficient data delivery and visualization techniques. The multidisciplinary simulation, estimation, and assimilation systems group at MIT (MSEAS) focuses on capturing and predicting diverse ocean dynamics, including physics, acoustics, and biology on varied scales, thereby developing new methods for multi-resolution ocean prediction and analysis, including data generation and assimilation. The group has primarily used non-interactive ocean plots to visualize its simulated and measured data. Although these maps and sections allow for analysis of ocean physics and the underlying numerical schemes, more interactive maps provide more user control over depicted data, allowing easier study and pattern identification on multiple scales. Integrating static and geospatial data in dynamic visualization creates a heightened viewpoint for analysis, enhances ocean monitoring and prediction, and contributes to building scientific knowledge. This thesis focuses on explaining the motivation behind and the methodologies applied in designing these interactive maps.

Thesis Supervisor: Pierre Lermusiaux
Title: Professor, Associate Department Head for Operations

Acknowledgments

First, I would like to express my deep gratitude to Professor Pierre Lermusiaux. Since he gave me the opportunity to join his MSEAS group, he offered nothing but patient guidance and useful advice towards the completion of the thesis. My grateful thanks are also extended to the members of the MSEAS group especially to Deepak Subramani, Corbin Foucart, Chris Mirabito and Wael H. Ali who welcomed me to the group and significantly contributed to the work. I would also like to extend my thanks to some amazing MIT people, who supported me over the years, namely Leslie Regan, Jason McKnight, Dean Staton, Prof Abeyaratne, Prof Karnik and Prof Hardt.

Second, I am blessed with an extraordinary group of people who have been and will always be there for me. Mike has been my main support in times of stress. Bardan has always rooted for me. Many thanks to Adham, Fadel, Ozzy, Assil, Dahlia, Taha, Leila, Khaled, Hens, I-95 and others.

Finally, I wish to thank my family for their support and encouragement throughout my studies. Thank you Salwa, Hussein, Qasim and Rana, Samer and Miriam, Sahar, and my three beautiful nieces, Reine, Rayan and Krystel.

*The MSEAS group is also grateful to the Office of Naval Research for support under Grants N00014-14-1-0725 (Bays-DA), N00014-14-1-0476 (Science of Autonomy LEARNS) and N00014-15-1-2616 (DRI-NASCar), to the National Science Foundation for support under grant EAR-1520825 (Hazards SEES - ALPHA), and to the Defense Advanced Research Projects Agency for support under Grant N66001-16-C-4003 (POSYDON-POINT), each to the Massachusetts Institute of Technology (MIT). We also thank the MIT Tata Center for their student support during the years 2017-2018.

Contents

List of Figures

Chapter 1

Motivation and Thesis Outline

1.1 Motivation

Data delivery and visualization software for ocean dynamics serves numerous purposes. They are tools by which ocean monitoring and forecasting products are distributed to end-users. These ocean products have a major impact on industries such as fisheries, coastal management, shipping, transport, marine recreation, maritime surveillance, and security [1] [2] [3]. Ocean data visualization software also depicts the chemical characteristics and quality of water in certain areas. They also help identify the potential for seabed mining and resource retention as the resources on the land are increasingly depleted. They can provide insights into the organic relationship between the biogeochemistry of the ocean and the weather and climate. Biological functioning modulates certain gases in the atmosphere, which influences its climate [4]. This influence is manifested in certain physical and biological processes that change in space and time and are often simulated using ocean observing and modeling systems. Moreover, ocean data provides the basis for innovative monitoring and mitigation of issues such as water pollution, oil spills, and loss of marine productivity [5] [6] [7] [8]. All these benefits also essentially drive scientific knowledge.

Although data collection/generation is the first step towards answering relevant questions, effective communication of data through visualization techniques renders complex multivariate data much more accessible. The MSEAS group at MIT generates different data variables using novel methods of multi-scale modeling and uncertainty quantification [9] [10] [11]. This data is often encoded in visual objects such as graphs, contour plots, or static maps (horizontal maps, cross-sections, etc.) [12] [13] [14]. Although these tools convey ideas effectively, interactive maps that serve user-specific purposes would provide more insight into such complex multi-resolution ocean data.

Since most of the generated data varies with time and space, dynamic maps have the advantage of capturing change in a very intuitive way. In addition to clearly communicating information, they stimulate user engagement by giving them the ability to control what they want to see and how they want to see it. For example, one could examine the time change of temperature in a certain ocean area using the features of one dynamic map that is fully interactive and allows multi-resolution views, as opposed to several static maps, each corresponding to a certain time of the day.

This thesis builds upon the power of interactive maps. It also sets up and builds the tools required for developing dynamic maps for ocean physics and uncertainty data generated in MSEAS, using and expanding upon existing open-source software.

1.2 Thesis Outline

Chapter 2 is a background review of the indispensable impact of oceans on the life on Earth. It highlights the organic relationship between ocean-related processes and other necessary phenomena of life such as moderation of weather and climate, ensuring biodiversity and symbiotic habitats, providing resources and raw materials, and mitigating global warming. It also explains the importance of studying oceans and data that characterize ocean physics, focusing on certain economic sectors and applications that could make the best use of such data.

Chapter 3 builds upon the profound power of data today and explains how this power is incomplete without effective communication of the data using good practices of data visualization. It describes the multi-scale equations and the uncertainty quantification models developed by the MSEAS group at MIT. It then depicts the need for interactive multilayered maps and compares their experience to more traditional infographics used by the MSEAS group such as snapshot images and static webpages.

Chapter 4 describes, in detail, the engineering process adopted in building the maps. This includes the educated selection of software, libraries, and plugins, and the placement of the maps within the MSEAS portal. Demonstrating examples of maps included in some MSEAS projects are also included.

Chapter 5 concludes the thesis and gives a brief insight into possible future enhancements of the methods, product and applications.

Bibliography

[1] P. F. J Lermusiaux, P. J. Haley, Jr, and N. K. Yilmaz. Environmental prediction, path planning and adaptive sampling: sensing and modeling for efficient ocean monitoring, management and pollution control. *Sea Technology*, 48(9):35–38, 2007.

[2] P. F. J. Lermusiaux, T. Lolla, P. J. Haley, Jr., K. Yigit, M. P. Ueckermann, T. Sondergaard, and W. G. Leslie. Science of autonomy: Time-optimal path planning and adaptive sampling for swarms of ocean vehicles. In Tom Curtin, editor, *Springer Handbook of Ocean Engineering: Autonomous Ocean Vehicles, Subsystems and Control*, chapter 21, pages 481–498. Springer, 2016.

[3] P. F. J. Lermusiaux, D. N. Subramani, J. Lin, C. S. Kulkarni, A. Gupta, A. Dutt, T. Lolla, P. J. Haley, Jr., W. H. Ali, C. Mirabito, and S. Jana. A future for intelligent autonomous ocean observing systems. *Journal of Marine Research*, 75(6):765–813, November 2017. The Sea. Volume 17, The Science of Ocean Prediction, Part 2.

[4] Lynn Margulis and J.e. Lovelock. Biological modulation of the earth's atmosphere. *Icarus*, 21(4):471–489, 1974.

[5] Pierre Lermusiaux, Patrick Haley, Wayne Leslie, Arpit Agarwal, Oleg Logutov, and Lisa Burton. Multiscale physical and biological dynamics in the philippine archipelago: Predictions and processes. *Oceanography*, 24(01):70–89, Jan 2011.

[6] Michela De Dominicis, Silvia Falchetti, Francesco Trotta, Nadia Pinardi, Luca Giacomelli, Ernesto Napolitano, Leopoldo Fazioli, Roberto Sorgente, Patrick J. Haley, Jr., Pierre F. J. Lermusiaux, F. Martins, and M. Cocco. A relocatable ocean model in support of environmental emergencies. *Ocean Dynamics*, 64(5):667–688, 2014.

[7] C. S. Kulkarni, P. J. Haley, Jr., P. F. J. Lermusiaux, A. Dutt, A. Gupta, C. Mirabito, D. N. Subramani, S. Jana, W. H. Ali, T. Peacock, C. M. Royo, A. Rzeznik, and R. Supekar. Real-time sediment plume modeling in the Southern California Bight. In *OCEANS Conference 2018*, Charleston, SC, October 2018. IEEE. In press.

[8] J. Coulin, P. J. Haley, Jr., S. Jana, C. S. Kulkarni, P. F. J. Lermusiaux, and T. Peacock. Environmental ocean and plume modeling for deep sea mining in the bismarck sea. In *Oceans 2017 - Anchorage*, Anchorage, AK, September 2017.

[9] Patrick J. Haley, Jr. and Pierre F. J. Lermusiaux. Multiscale two-way embedding schemes for free-surface primitive equations in the "Multidisciplinary Simulation, Estimation and Assimilation System". *Ocean Dynamics*, 60(6):1497–1537, December 2010.

[10] P. J. Haley, Jr., A. Agarwal, and P. F. J. Lermusiaux. Optimizing velocities and transports for complex coastal regions and archipelagos. *Ocean Modeling*, 89:1–28, 2015.

[11] P. F. J. Lermusiaux, C.-S. Chiu, G. G. Gawarkiewicz, P. Abbot, A. R. Robinson, R. N. Miller, P. J. Haley, Jr, W. G. Leslie, S. J. Majumdar, A. Pang, and F. Lekien. Quantifying uncertainties in ocean predictions. *Oceanography*, 19(1):92–105, 2006.

[12] Suzana Djurcilov, Kwansik Kim, Pierre F. J. Lermusiaux, and Alex Pang. Volume rendering data with uncertainty information. In David S. Ebert, Jean M. Favre, and Ronald Peikert, editors, *Data Visualization 2001*, Joint Eurographics - IEEE TCVG Symposium on Visualization, pages 243–252, 355–356. Springer Vienna, 2001.

[13] Suzana Djurcilov, Kwansik Kim, Pierre Lermusiaux, and Alex Pang. Visualizing scalar volumetric data with uncertainty. *Computers and Graphics*, 26(2):239–248, 2002.

[14] Arkopal Dutt, Deepak N. Subramani, Chinmay S. Kulkarni, and Pierre F. J. Lermusiaux. Clustering of massive ensemble of vehicle trajectories in strong, dynamic and uncertain ocean flows. In *OCEANS Conference 2018*, Charleston, SC, October 2018. IEEE. In press.

Chapter 2

Background

2.1 Oceans Keep Us Alive

Oceans cover 71% of Earth's surface [1] and contain 97% of the water available on the planet [2]. They have been always recognized as one of the most important natural resources. Their diverse habitats and ecological systems host 99% of the living space on Earth [3]. In oceans, life stretches from the epipelagic surfaces - where enough sunlight penetrates for photosynthesis [4] - to extreme environments in the hadal zone, tens of thousands of feet below the surface. Figure 2-1 depicts the different ocean zones.

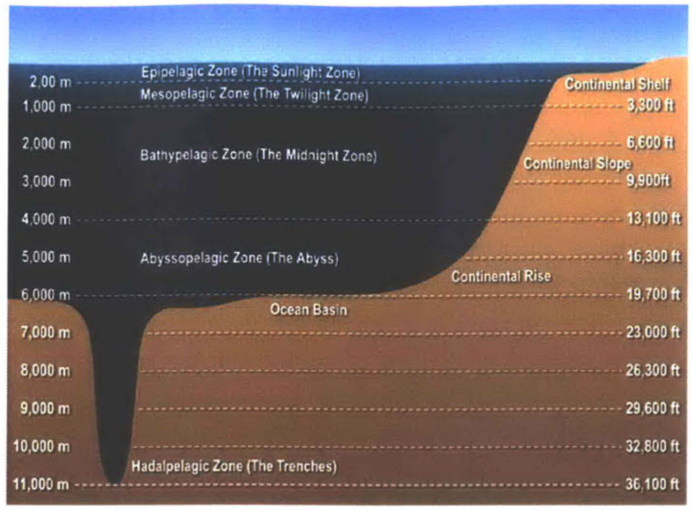

Figure 2-1: Ocean Zones [5]

The profound value of oceans is not only ecological but also extends to economic and social impact [3]. However, in order to better understand how oceans affect us, optimize the sustainable use of their resources and act on hazardous trends, **it is crucial to measure, model and visualize ocean data**.

In his opening remarks to the Ocean Conference (Sweden and Fiji, June 2017), the UN Secretary General António Guterres called for a coordinated international effort to mitigate the intensity of the threat on oceans given the rising sea levels, climate change, pollution and overfishing. His global action list emphasized that we must deepen our knowledge base, with better data, information and analysis because *we simply cannot improve what we do not measure.* [6]

2.2 The Significance of Ocean Data

In this chapter, we discuss some of the biological, physical, economic and social interactions that necessitate the study of ocean dynamics.

2.2.1 Climate and Weather

Oceans regulate Earth's climate and define its different weather zones, which makes this planet habitable. Without oceans, weather zones would be more extreme [7]. Therefore, understanding ocean physics is extremely important especially amid the increasing risks of climate change and the accompanying disasters such as hurricanes, floods, droughts, heat waves, and melting glaciers. Not only do oceans store the majority of solar radiation but also contribute to the even distribution of heat around the globe.

First, oceans are a major player in the hydrological cycle on Earth [8]. Solar heat causes water at the surface of the ocean to evaporate. Water vapor then rises and condenses as clouds that are driven by trade winds and cause rain and storms elsewhere on land. Therefore, oceans facilitate the continuous movement of water. The deep understanding of the ocean's properties translates into more control over this cycle that is a guarantee for life for many species.

Second, oceans facilitate the thermohaline circulation by distributing heat and salt around the globe [1]. Two forces mainly drive ocean circulation. These are wind stress - manifested by surface winds due to Ekman spirals - and buoyancy flux between atmosphere and ocean [9] - controlled by temperature and salinity gradients and the subsequent density stratification. Although wind-driven forces seem to be more vigorous than buoyancy in regulating the redistribution of salt and heat in the upper kilometers, buoyancy effect is full-depth and often involves ocean overturning that translates into a direct effect on climate [10]. Ocean currents that often trace the coastlines, act as massive heat belts that moderate global climate by carrying heat from one zone to another. For instance, they can transport warm water and precipitation from the equator towards the poles and cold water from the poles back to the tropics [11].

Third, vertical motions in the ocean are critical to the exchange of heat and gases such as CO_2 between the surface layer and the deep ocean. Processes such as upwelling take place in the ocean. Dense, cooler, more nutrient-rich water travels up from the deep ocean to replace the warmer, nutrient-depleted surface water [12]. This phenomenon is crucial for many biological processes that conserve several marine ecosystems.

The study and visualization of ocean data in a way that demonstrates trends in parameters such as temperature, salinity and stress largely contribute to better understanding of the described cycles and more effective mitigation of potential calamities.

2.2.2 Carbon Sequestration

Oceans play a key role in the carbon cycle as they take up a large percentage of atmospheric CO_2 [13]. Carbon dioxide hydrates are an effective vehicle for deep ocean carbon sequestration [14]. These hydrates are typically denser than seawater, so they naturally sink to the deep ocean while dissolving, which facilitate dispersion.

Burning fossil fuels has accumulated carbon dioxide in the atmosphere, which exacerbates the greenhouse effect. Oceans have always captured a part of the atmospheric carbon. However, this cycle is not infinite. One NASA model has shown that doubling the level of pre-industrial CO_2 increases the ocean's carbon content, but as water temperature increases, its ability to dissolve CO_2 drops [15]. This drop accumulates more CO_2 in the atmosphere, which causes a rise in temperature.

The global oceans are connected by deep currents and surface currents. Carbon from the atmosphere enters the ocean depths in areas of deep water formation in the North Atlantic and offshore of the Antarctic Peninsula. Where deep currents rise towards the surface, they can release carbon dioxide stored centuries ago [16]. This is shown in Figure 2-2

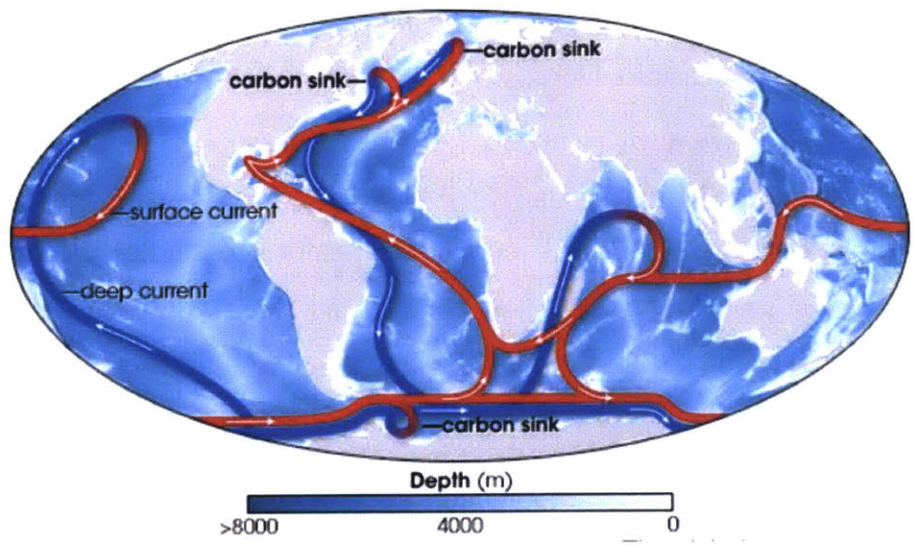

Figure 2-2: Ocean Carbon Cycle [16]

In addition to deep injection, priming the biological pump by iron fertilization of the ocean is another approach to sequester carbon. Iron stimulates the production of phytoplanktons, which leads to an algal bloom that nourishes sea organisms and eventually accelerates CO_2 dissolving [17].

Therefore, it is important to characterize seawater properties and model its temperature, salinity and alkalinity in order to quantify the water's ability to dissolve CO_2 and mitigate global warming.

2.2.3 Resources

Oceans are a large source of a number of human necessities. This includes - but is not limited to- food, oil and gas, energy, salt, sand, gravel, minerals and other commercially important materials such as diamond, manganese, copper and nickel [18].

It has become apparent that seabed mining carries a lot of potential to supply dwindling resources needed by humans. With this discovery, a number of questions about the impact of deep-sea mining arose, especially related to its effect on the ocean's ecosystems and the circulation of deep ocean pollutants [19]. Deep sea-mining activities are being largely studied and it is unequivocally important to model ocean dynamics during these studies.[20]

In one of the MSEAS activities, namely plume modeling for deep sea mining in the Bismarck sea[19], the MSEAS relied on a number of models to carry out the experiment. The modeling capabilities included implicit two-way nesting for multi-scale hydrostatic primitive equation (PE) dynamics with a nonlinear free-surface and a high-order finite element code on unstructured grids for non-hydrostatic processes [21] [22] [23] [24]. Additional subsystems included Lagrangian Coherent Structures, non-Gaussian data assimilation and adaptive sampling.

2.2.4 Economy and Society

Currently, 40% of the world's population inhabits coastal regions (United Nations, 2015) and and over 3 billion people depend directly on marine resources for livelihoods and welfare [25]. The services provided by the oceanic ecological systems contribute significantly to welfare and therefore represent a big portion of the economic value of the planet [3]. Coastal environments, including estuaries, coastal wetlands, beds of sea grass and algae, coral reefs, and continental shelves cover only 6.3% of the world's surface, but are responsible for 43% of the estimated value of the world's ecosystem services [26]. Preserving this economic value is crucially important to alleviate poverty and provide job opportunities. Sustainable governance of these systems necessitate accurate modeling of coastal oceanic regions. *In fact, the coastal ocean is a prime example of multi-scale nonlinear fluid dynamics* [25].

The economic value of the oceans is inextricably linked to social welfare. The social importance of the oceans for global transportation and as a unifying element in the cultures of many coastal countries cannot be overstated [3].

Some of the economic verticals that would make great use of ocean data models are:

a. **Fisheries**

Modeling and visualizing ocean physics by fisheries are necessary tools for optimal management of fisheries and sustainable seafood supply. Overfishing has been one of the most problematic issues oceans face as it depletes the adult fish population in some regions [27]. Approximately 57% of fish stocks are fully-exploited and 30% over-exploited, depleted or recovering [28].

Multi-scale modeling of coastal oceans involves study of ocean fields and their uncertainties and coastal ecosystem-based scenario analyses that help fisheries make better technical decisions about their fishing methods and the frequency they fish at. In addition, ocean data helps design more complex systems that optimize guidance sensors for boats. It also helps understand changes in the characteristic quality of fishes in terms of their plasma chloride levels and muscle tissue moisture.

b. **Energy**

A number of marine renewable energy technologies have tested to be promising (shown in Figure 2-3). Although these technologies are at their early stage of development, they are expected to grow. Globally, the renewable energy sector between 2004 and 2013, increased from 85 to 560 GW (led by the wind industry) [29].

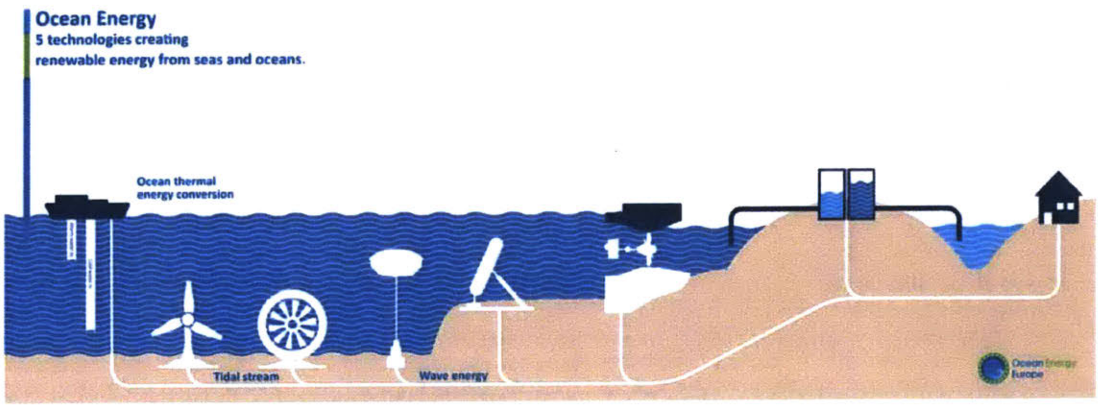

Figure 2-3: Marine Energy Technologies [30]

With the urgency of providing a sustainable future for the Earth, ocean energy sources prove to be necessary. As solar radiation is converted to wind energy and later wave energy, the amount of energy per unit volume becomes more concentrated [31]. Therefore, considering that waves are an intensified form of wind energy that is capable to travel long distances with minimal losses, the wave energy sector is expected to grow till it equals the importance of offshore wind energy.

The ocean hosts a number of energy extraction options [32]. Examples include (1) wave energy technologies that use of ocean swells created by persistent winds [29], (2) tidal energy technologies that garner the energy effect of the pull between the moon and the sun in the motion of tides, (3) current energy systems that capture the enormous amount of energy contained in ocean currents, thanks to the water density, (4) salinity gradient systems such as reverse electrodialysis and pressure retarded osmosis, and (5) thermal gradient systems that run a heat engine between shallow and deep ocean levels.

The study and development of the potential of these energy sources necessitate the knowledge of the temporal and spatial variations of the ocean physics.

c. **Maritime Security and Surveillance**

The development of comprehensive and real-time systems, targeted towards surveillance and security in marine regions, requires advanced accurate multi-scale ocean modeling. For instance, geospatial sound speed models are extremely helpful in detection of underwater objects and contribute to long-range low-frequency acoustical research [33] [34] [35].

d. **Other sectors**

Other sectors that largely rely on ocean data include tourism (in which temperature, salinity and ocean current profiles impact the type of recreational activities to be established), shipping, coastal management serviced to protect against flood and erosion, hazard prediction analyses, and development of advanced systems such as underwater navigation and autonomous vehicles.

Hence, ocean dynamics data are undeniably crucial for the betterment of science, economies, and societies in general.

Bibliography

[1] Stefan Rahmstorf. Ocean circulation and climate during the past 120,000 years. *Nature*, 419(6903):207–214, Dec 2002.

[2] NOAA. Where is all of the earth's water?: https://oceanservice.noaa.gov/facts/wherewater.html. *NOAA's National Ocean Service*, Dec 2009.

[3] Robert Costanza. The ecological, economic, and social importance of the oceans. *Ecological Economics*, 31(2):199–213, 1999.

[4] Weimin Gao, Xu Shi, Jieying Wu, Yuguang Jin, Weiwen Zhang, and Deirdre R. Meldrum. Phylogenetic and gene expression analysis of cyanobacteria and diatoms in the twilight waters of the temperate northeast pacific ocean. *SpringerLink*, Jun 2011.

[5] J.D. Knight. Layers of the ocean - deep sea creatures on sea and sky: http://www.seasky.org/deep-sea/ocean-layers.html.

[6] United Nations. Secretary-general's opening remarks to the ocean conference (sweden and fiji), 2017: https://www.un.org/sg/en/content/sg/statement/2017-06-05/secretary-generals-opening-remarks-ocean-conference-delivered.

[7] NOAA. How does the ocean affect climate and weather on land?: https://oceanexplorer.noaa.gov/facts/climate.html. *Deepwater Exploration of the Marianas RSS*, Jun 2013.

[8] Moustafa T. Chahine. The hydrological cycle and its influence on climate. *Nature*, 359(6394):373–380, 1992.

[9] M.f. Cronin and J. Sprintall. Wind and buoyancy-forced upper ocean. *Encyclopedia of Ocean Sciences*, page 3219–3226, 2001.

[10] Andrew Revkin. *Global Warming: Understanding the Forecast.* Abbeville Press, 1992.

[11] Wallace Broeker. The great ocean conveyor. *Oceanography*, 4(2):79–89, 1991.

[12] T Sarhan. Upwelling mechanisms in the northwestern alboran sea. *Journal of Marine Systems*, 23(4):317–331, 2000.

[13] Roger Revelle and Hans E. Suess. Carbon dioxide exchange between atmosphere and ocean and the question of an increase of atmospheric co2 during the past decades. *Tellus*, 9(1):18–27, 1957.

[14] Olivia R. West, Costas Tsouris, Sangyong Lee, Scott D. Mccallum, and Liyuan Liang. Negatively buoyant co2-hydrate composite for ocean carbon sequestration. *AIChE Journal*, 49(1):283–285, 2003.

[15] J. G. Canadell, C. Le Quere, M. R. Raupach, C. B. Field, E. T. Buitenhuis, P. Ciais, T. J. Conway, N. P. Gillett, R. A. Houghton, G. Marland, and et al. Contributions to accelerating atmospheric co2 growth from economic activity, carbon intensity, and efficiency of natural sinks. *Proceedings of the National Academy of Sciences*, 104(47):18866–18870, 2007.

[16] NASA. The carbon cycle: : https://earthobservatory.nasa.gov/features/carboncycle.

[17] K H Coale, K S Johnson, S E Fitzwater, R M Gordon, S Tanner, F P Chavez, L Ferioli, C Sakamoto, P Rogers, F Millero, and et al. A massive phytoplankton bloom induced by an ecosystem-scale iron fertilization experiment in the equatorial pacific ocean. *Nature.*, Oct 1996.

[18] P. A. Rona. Geology: Resources of the sea floor. *Science*, 299(5607):673–674, 2003.

[19] J. Coulin, P. J. Haley, Jr., S. Jana, C. S. Kulkarni, P. F. J. Lermusiaux, and T. Peacock. Environmental ocean and plume modeling for deep sea mining in the bismarck sea. In *Oceans 2017 - Anchorage*, Anchorage, AK, September 2017.

[20] C. S. Kulkarni, P. J. Haley, Jr., P. F. J. Lermusiaux, A. Dutt, A. Gupta, C. Mirabito, D. N. Subramani, S. Jana, W. H. Ali, T. Peacock, C. M. Royo, A. Rzeznik, and R. Supekar. Real-time sediment plume modeling in the Southern California Bight. In *OCEANS Conference 2018*, Charleston, SC, October 2018. IEEE. In press.

[21] Patrick J. Haley, Jr. and Pierre F. J. Lermusiaux. Multiscale two-way embedding schemes for free-surface primitive equations in the "Multidisciplinary Simulation, Estimation and Assimilation System". *Ocean Dynamics*, 60(6):1497–1537, December 2010.

[22] P. J. Haley, Jr., A. Agarwal, and P. F. J. Lermusiaux. Optimizing velocities and transports for complex coastal regions and archipelagos. *Ocean Modeling*, 89:1–28, 2015.

[23] M. P. Ueckermann and P. F. J. Lermusiaux. Hybridizable discontinuous Galerkin projection methods for Navier–Stokes and Boussinesq equations. *Journal of Computational Physics*, 306:390–421, 2016.

[24] C. Foucart, C. Mirabito, P. J. Haley, Jr., and P. F. J. Lermusiaux. Distributed implementation and verification of hybridizable discontinuous Galerkin methods for nonhydrostatic ocean processes. In *OCEANS Conference 2018*, Charleston, SC, October 2018. IEEE. In press.

[25] Deepak Narayanan Subramani. *Probabilistic regional ocean predictions: stochastic fields and optimal planning.* 2018.

[26] Mostafa Kamal Tolba. *Our fragile world: challenges and opportunities for sustainable development.* Eolss, 2001.

[27] E. S. Russell. Some theoretical considerations on the "overfishing" problem. *ICES Journal of Marine Science*, 6(1):3–20, 1931.

[28] David J. Attard, Malgosia Fitzmaurice, and Alexandros X. M. Ntovas. *The IMLI treatise on global ocean governance: UN specialized agencies and global ocean governance Volume II.* Oxford University Press, 2018.

[29] Eugen Rusu and Florin Onea. A review of the technologies for wave energy extraction. *Clean Energy*, 2(1):10–19, Jul 2018.

[30] EnergyWall. Ocean energy: http://energywall.in/ocean-energy. Mar 2018.

[31] Australian Academy of Science. Harnessing the power of the ocean: https://www.science.org.au/curious/technology-future/ocean-power. Sep 2017.

[32] S. Deluca, S. Zanforlin, B. Rocchio, P. J. Haley, C. Foucart, C. Mirabito, and P. F. J. Lermusiaux. Scalable coupled ocean and water turbine modeling for assessing ocean energy extraction. In *OCEANS Conference 2018*, Charleston, SC, October 2018. IEEE. In press.

[33] A. R. Robinson and P. F. J. Lermusiaux. Prediction systems with data assimilation for coupled ocean science and ocean acoustics. In A. Tolstoy et al, editor, *Proceedings of the Sixth International Conference on Theoretical and Computational Acoustics*, pages 325–342. World Scientific Publishing, 2004. Refereed invited Keynote Manuscript.

[34] Pierre F. J. Lermusiaux, Jinshan Xu, Chi-Fang Chen, Sen Jan, L.Y. Chiu, and Yiing-Jang Yang. Coupled ocean–acoustic prediction of transmission loss in a continental shelfbreak region: Predictive skill, uncertainty quantification, and dynamical sensitivities. *IEEE Journal of Oceanic Engineering*, 35(4):895–916, October 2010.

[35] Frans-Peter A. Lam, Patrick J. Haley, Jr., Jeroen Janmaat, Pierre F. J. Lermusiaux, Wayne G. Leslie, Mathijs W. Schouten, Lianke A. te Raa, and Michel Rixen. At-sea real-time coupled four-dimensional oceanographic and acoustic forecasts during Battlespace Preparation 2007. *Journal of Marine Systems*, 78(Supplement):S306–S320, November 2009.

Chapter 3

MSEAS Ocean Data Visualization

The development of appropriate data visualization tools must be based upon deep understanding of the nature of the data, the relationship among different data sets, the desired features, and the user expectations. The design of our ocean dynamics maps is based upon the models developed by the Multidisciplinary Simulation, Estimation, and Assimilation Systems (MSEAS) group at MIT. In this chapter, we start from the research activities and visualization tools of MSEAS and expand to data visualization features that reflect an enhancement of the current tools.

3.1 MSEAS

MSEAS is a research group, focused on regional ocean data assimilation and led by Professor Pierre Lermusiaux. The group creates and utilizes new methods for multi-scale modeling, uncertainty quantification, data assimilation and the guidance of autonomous vehicles. These advances are then utilized to better understand physical, acoustical and biological interactions [1].

The group hosts an extensive list of ocean-related research projects and adopts an integrated approach to characterize complex fluid systems and develop computational models for prediction and quantification of ocean dynamics. The group is also involved in several sea exercises that test and validate the theory. Machine learning techniques are then applied to enhance the theoretical models. Within data assimilation, a number of techniques are applied. Examples include direct multi-scale filtering and smoothing, multi-resolution data assimilation and scale-decomposition, and multi-scale adaptive sampling and modeling.

3.2 MSEAS Data Cycle

3.2.1 Data Discovery

Any data cycle starts with mining the data and understanding a potential strategy for a story. Data mining involves numerical computation or experimental results. The MSEAS group has mastered the data discovery applications starting from their PE model, described below.

PE Model

The MSEAS group utilizes their stochastic ocean PE model that mainly solves a set of nonlinear high-order partial differential equations called Primitive Equations (PE) [2]. Primitive equations are typically conservation equations of mass, momentum and thermal energy. These equations are constrained by a set of initial conditions, boundary conditions, and forcing parameters. The model output consists of a set of prognostic variables that are governed by time evolution equations, and diagnostic variables that are non-prognostic. In order to test and validate the PE model, MSEAS also works with real ocean data because data motivates discoveries and fosters new fundamental ideas.

Data Fields

In the context of map design, it is important to understand the nature of the forecasted ocean dynamics. The data variables intended to visualize are:

a. **Ocean Physics**

These are the fields that vary spatiotemporally and are a result of numerical solutions of the PE model. These data fields are divided among:

1. **Scalar Fields**

   These fields are parameter distributions in space, whose values at each point - defined by an intersection of a latitude line, longitude line and a depth level- are scalar quantities. Examples include:

   - **Temperature**: Temperature is a prognostic variable, computed using the first law of thermodynamics [after solving Navier-Stoke's (balance of momentum) equation for the horizontal and vertical velocity fields].
   - **Salinity**: Salinity is a prognostic variable, computed using a conservation of salt equation that takes into account the turbulent sub-gridscale processes.
   - **Density**: Density is a diagnostic variable that has an equation of state, as a function of temperature and salinity profiles.
   - **Surface Elevation**: Surface elevation is a prognostic variable defined at the ocean's surface relative to a zero line.
   - **Speed of Sound**

2. **Vector Fields**

   These fields assign a vector for each point in the domain. These vectors have a direction, an angle relative to a reference line, and a magnitude, that can be shown as a scalar field. Vector fields shown in our maps are:

   - **Velocity**: Velocity is a prognostic variable that results from the solution of conservation of momentum equations.
   - **Barotropic velocity**: The barotropic velocity field is computed by vertical integration of the horizontal momentum, and thus characterizes the component of the total velocity that is related to horizontal transport and to changes in the ocean surface. It is depth independent.

3. **Secondary Vector Fields**

These include fields such as **vorticity** that represents the local spinning motion of continuum in the defined domains.

b. **Ocean Uncertainties**

Because of limitations in measurement, there are varying degrees of uncertainty in the initial conditions, boundary conditions, forcing parameters and even in the parametrization of the partial differential equations. This necessitates the development of rigorous models that make fundamental probabilistic predictions and quantify uncertainty fields [3] [4] [5]. For now, our new interactive maps will show **mean** and **standard deviation** fields of the statistics characterizing ocean physics described in the previous section.

c. **Other Ocean Fields**

Other fields - that do not fall under ocean physics and their uncertainties - could be routes for optimal path planning or Lagrangian coherent structures that show complex ocean patterns especially in hazardous event studies.

3.2.2 Data Visualization

Data visualization follows data mining and it aims at effectively communicating data to users. Data visualization tools are expected to process the information that emerges out of the data discovery phase and present them in a user-friendly fashion.

An estimated 2.5 billion gigabytes of data is generated on a daily basis [6]. The overwhelming growth of data generation has necessitated parallel development of effective data visualization tools. There are a number of theories that describe what is a good practice in visualizing data. However, it is easy to realize that good data visualization allows quick access and deep insight into data. It converts large complex sets of data into simple, easily digestible visuals. It also enables the user to recognize trends and patterns, and maybe act on them. Multilayering is a powerful tool that helps user establish hierarchies and understand the relationship between different variables. In a broader perspective, good data visualization tools foster a new language that facilitate quick, yet insightful, decision making.

MSEAS Data Visualization

The MSEAS PE Model output variables have been typically visualized using static plots. These plots are different types of graphics (e.g. color maps, contour plots, quiver plots) produced in MATLAB or traditional fortran-based NCAR graphics [7].

For example, in one project (NSF-ALPHA [8]), MSEAS plots include horizontal maps at different depths or vertical sections along different lines of (1) scalar fields such as temperature, uncertainty in temperature, salinity, and magnitude of velocity, or (2) vector fields such as velocity vectors, or (3) secondary vector fields such as vorticity. Other examples include plots of the backward and forward finite-time Lyapunov exponent (FTLE) fields at different depths, drifter trajectories, buoy data vs. atmospheric data, time-averaged HF Radar velocities, and horizontal maps of atmospheric products such as wind velocity, air temperature, and other atmospheric fluxes and stresses. In other projects, additional fields are plotted such as the speed of sound in vertical sections and horizontal maps at different zoom levels (POSYDON-POINT [9]), or glider reachability fronts in large domains and zooms in the Arabian Sea (NASCar-OPS [10] [11]).

Some examples are included in Figure 3-1. Although these are simple and powerful graphics, they show limited capabilities relative to maps that allow high resolution zooming and panning.

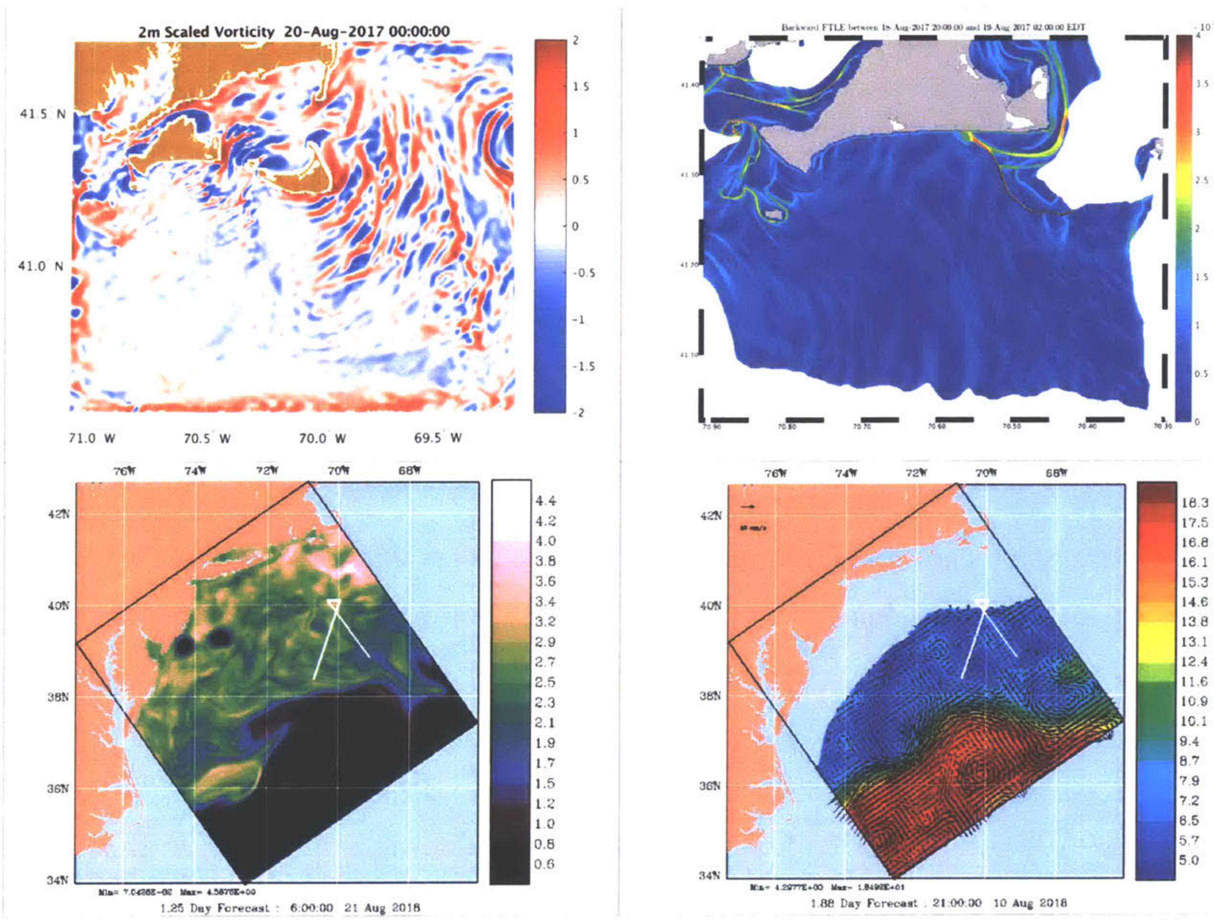

Figure 3-1: Ocean Dynamics Examples - top left: vorticity profile (NSF-ALPHA 2017), top right: Backward FTLE profile (NSF-ALPHA 2017), bottom left: standard deviation of sound speed field (POSYDON-POINT 2018), bottom right: temperature profile (POSYDON-POINT 2018) [12]

3.2.3 Web Experience

In today's world, it has become important to complement visually engaging data visualization tools with an effective web experience that completes the data story. The importance of a web tool lies in providing the user with a fast, simple but powerful data-driven experience, that is easy to comprehend and share. Whether it is a website or a mobile application, an effective web experience must challenge the user to think about the data substance rather than about the tools used to build the visualization.

The MSEAS website has provided a serial web experience that allows the user to access the plots - similar to the examples of Figure 3-1. However, the experience of the user is not made easy or intuitive as they cannot make direct conclusions and recognize trends that should be obvious.

In order to showcase this experience, consider the following example. Suppose an ocean enthusiast is interested in the POSYDON-POINT sea exercise carried out by MSEAS in the mid-Atlantic. Let's say the user is seeking information about the horizontal temperature distribution in the exercise's full domain at a depth of 100 m, on February 26^{th}, 2017 at 9 a.m. In order to retrieve this information using the MIT MSEAS web, the user must follow the following steps:

- **Step 1**: navigate to the MIT MSEAS Sea Exercises webpage and select the POSYDON-POINT 2017 sea exercise. The Sea Exercises page lists the different sea activities the MSEAS group is involved in to test and validate the models developed in theory. A snapshot of the page is shown in Figure 3-2.

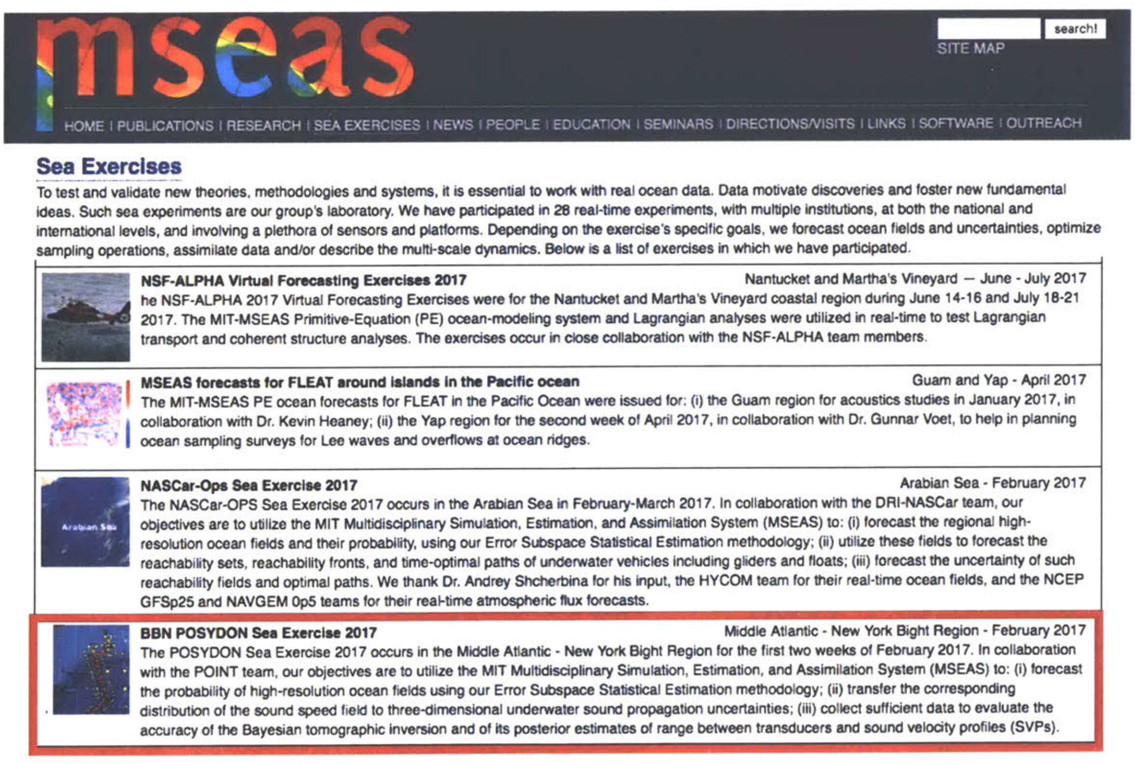

Figure 3-2: Sea Exercises [1]

- **Step 2**: navigate to the POSYDON POINT calendar. In this page, the date and type of data can be selected. In this example, the user selects a central forecast showing a horizontal map on February 26^{th}, 2017 as shown in Figure 3-3.

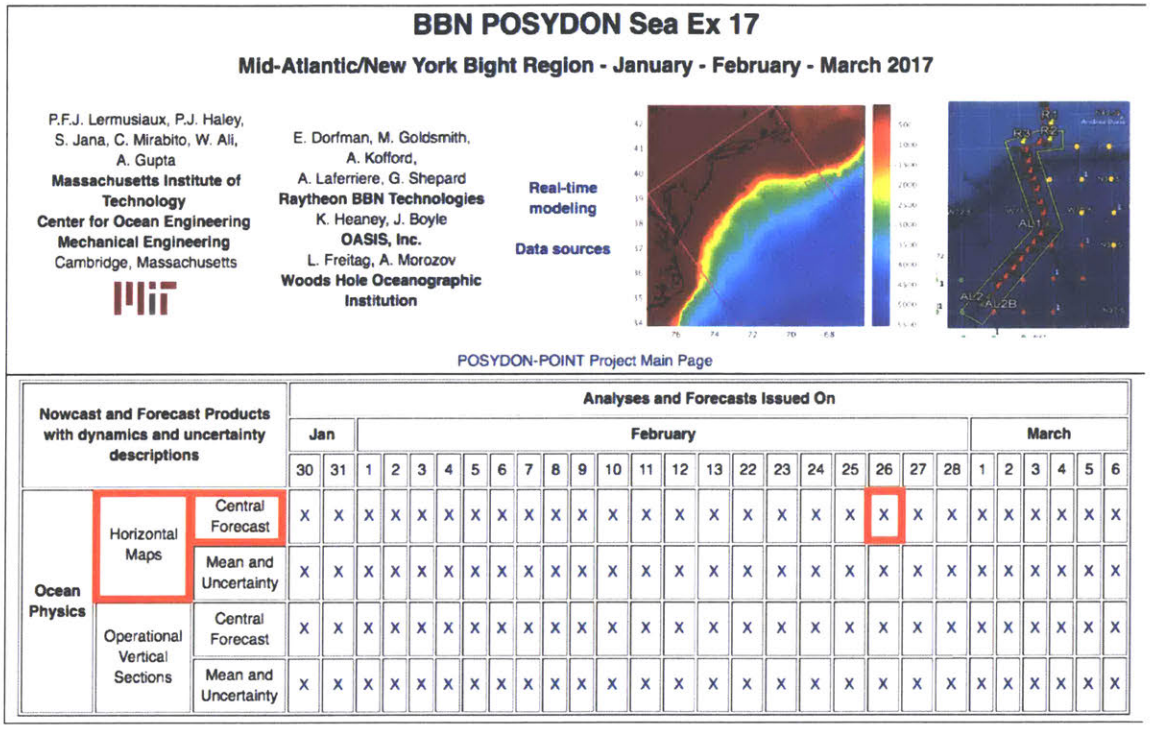

Figure 3-3: POSYDON-POINT Calendar [1]

- **Step 3**: select the corresponding domain and depth. This page arranges data according to the domain of interest (full domain or zoomed area) and depth below the surface of the ocean. In this example, the user selects full-domain and 100 m depth as shown in Figure 3-4.

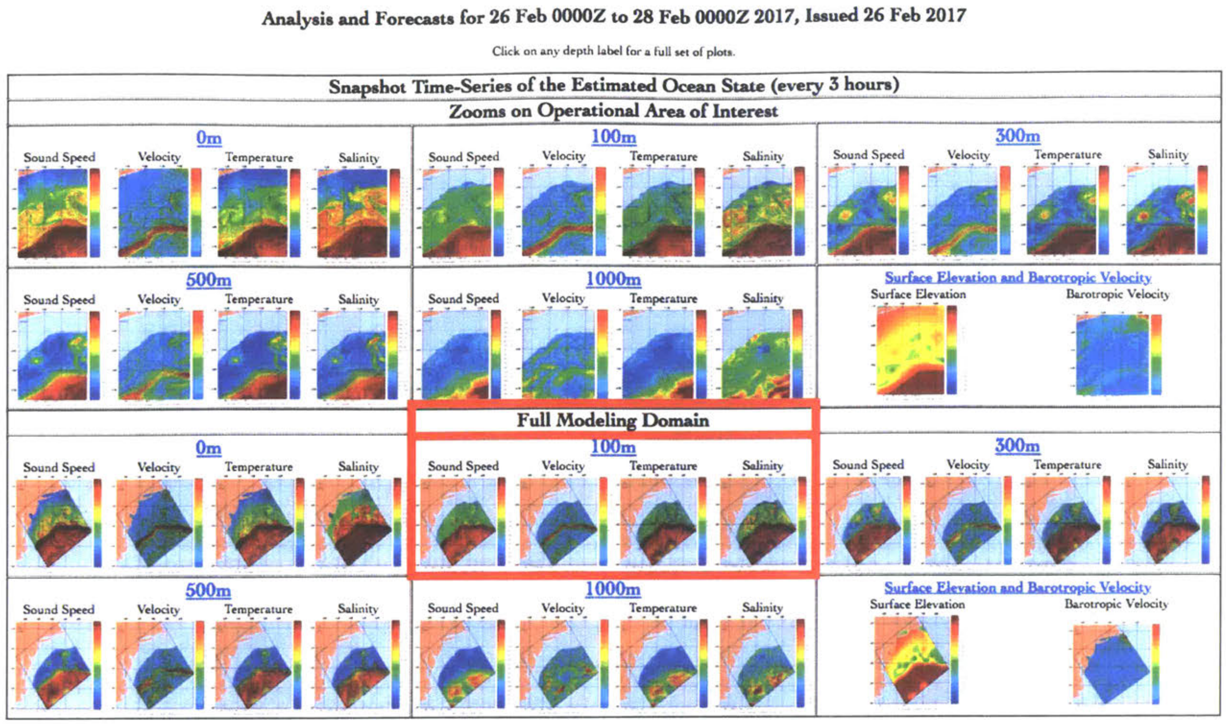

Figure 3-4: Domain and Depth [1]

- **Step 4**: select the desired data variable. This page lists the different modeled data fields, namely sound speed, velocity, temperature and salinity in this specific exercise. In this example, the user selects temperature as shown in Figure 3-5.

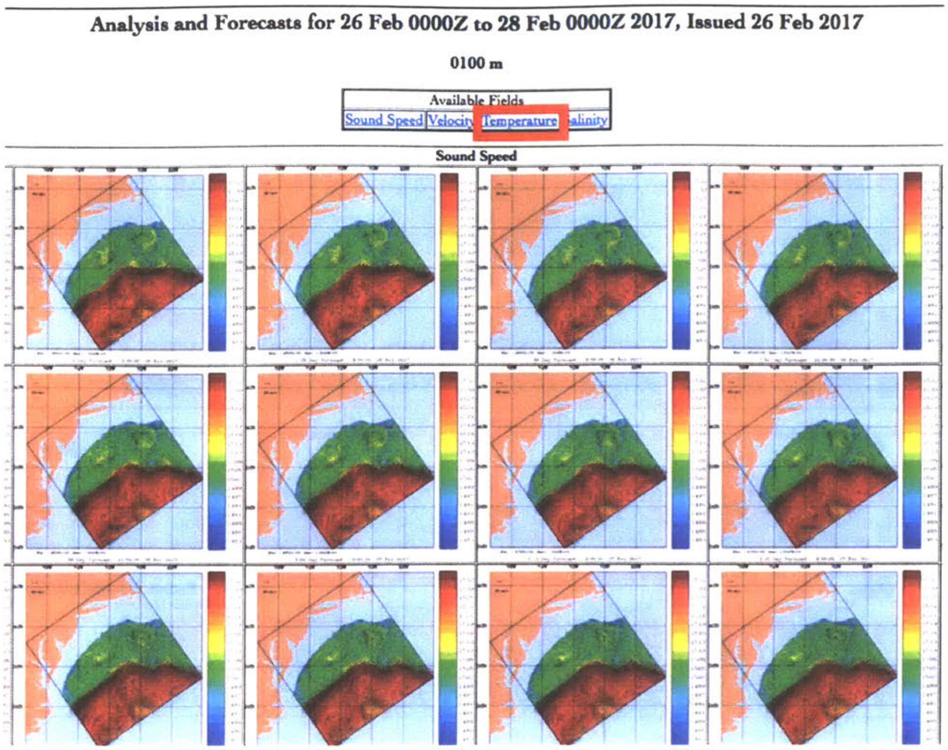

Figure 3-5: Data Variable [1]

- **Step 5**: select the desired time. This page arranges the temperature maps by their time stamp. The difference between each two consecutive thumbnails correspond to a period of 3 hours. In this example, the user selects the fifth thumbnail because the first one corresponds to 00:00 a.m. and they are interested in the profile at 9 a.m. The selected time thumbnail is shown in Figure 3-6.

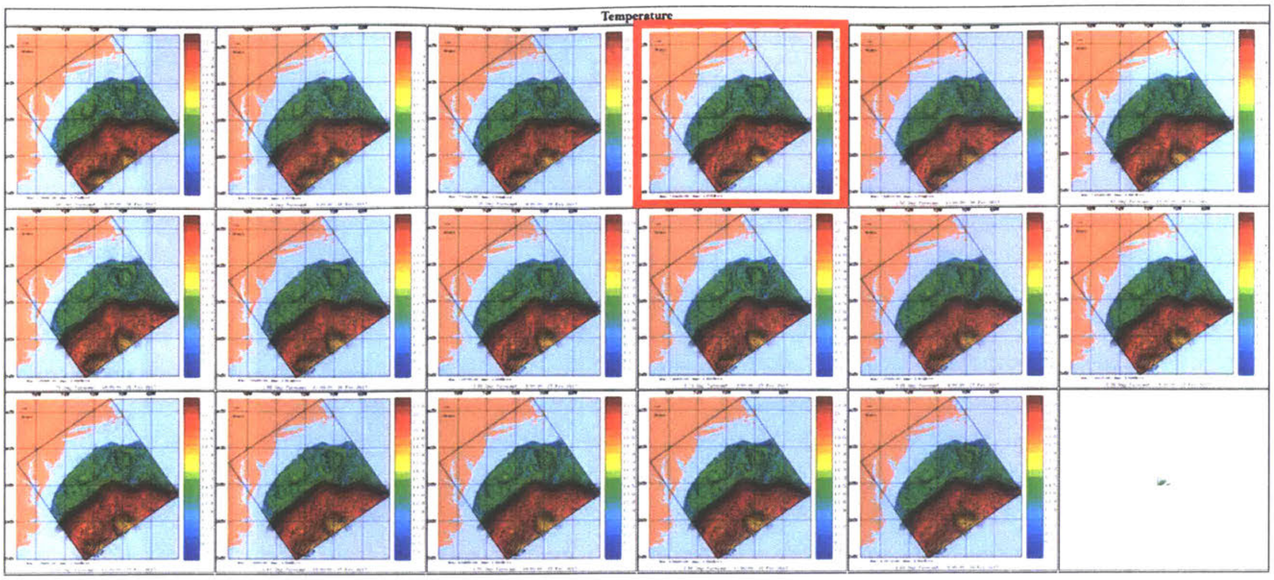

Figure 3-6: Time Thumbnails [1]

- **Step 6**: visualize the data. This page shows a png (portable networks graphic) or a graphics interchange format (gif) generated by MATLAB or NCAR. The graphic plots a colormap of the temperature field in the full domain. It also features a date and time stamp, longitude and latitude lines, extrema information, and a well-defined color legend. The image of this example is shown in Figure 3-7.

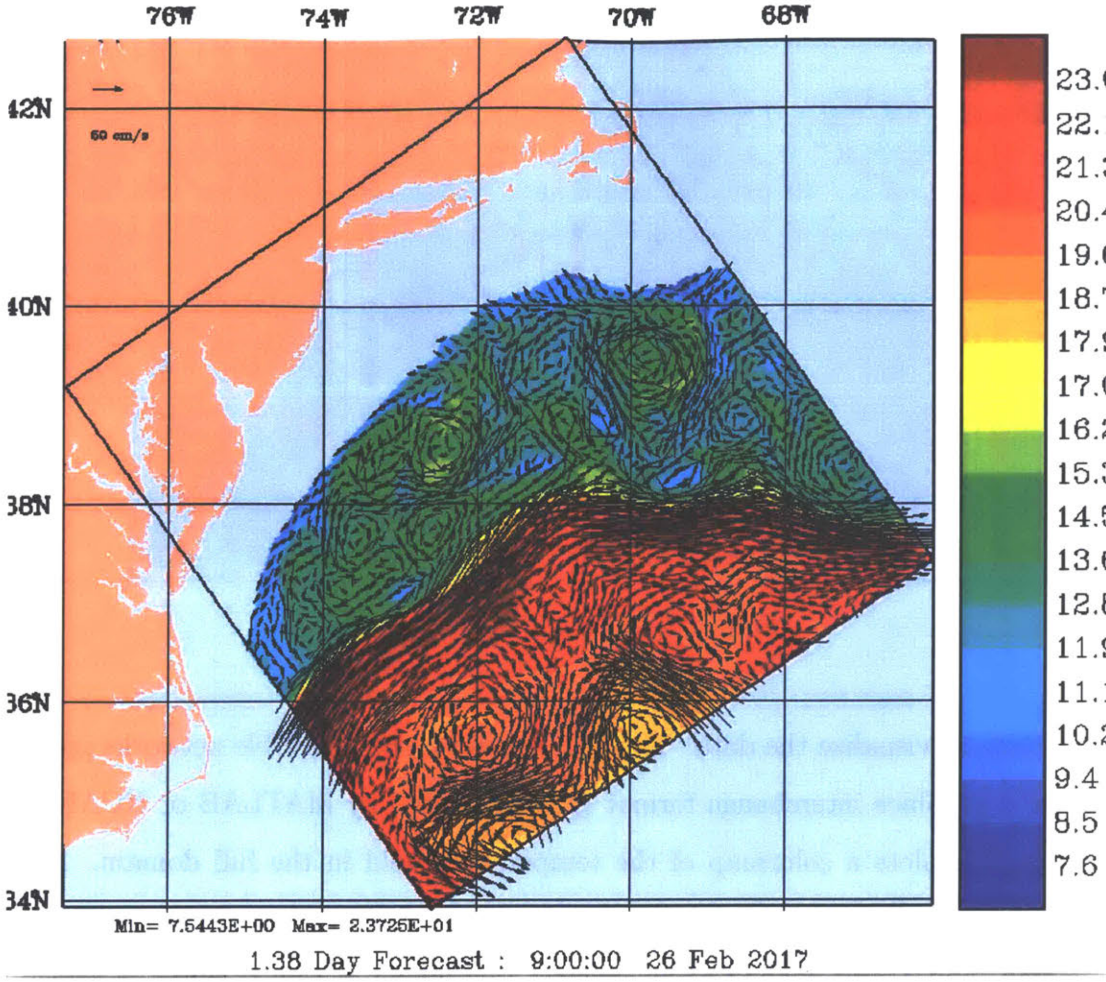

Figure 3-7: Desired Temperature Field [1]

As we have seen, the web experience is not very friendly as the user must return to different webpages if they're interested in changing a parameter such as time, depth, or the desired field. This necessitates a more intuitive approach that captures variables in a multi-layered platform and allows the user to make quick conclusions. *This is why we designed user-controlled multi-layered multi-variable web maps.*

Bibliography

[1] Multidisciplinary Simulation Estimation and MIT Assimilation Systems MSEAS. http://mseas.mit.edu/.

[2] Deepak Narayanan Subramani. *Probabilistic regional ocean predictions: stochastic fields and optimal planning.* 2018.

[3] P. F. J. Lermusiaux. Uncertainty estimation and prediction for interdisciplinary ocean dynamics. *Journal of Computational Physics*, 217(1):176–199, 2006.

[4] Pierre F. J. Lermusiaux, P. Malanotte-Rizzoli, D. Stammer, J. Carton, J. Cummings, and A. M. Moore. Progress and prospects of U.S. data assimilation in ocean research. *Oceanography*, 19(1):172–183, 2006.

[5] P. F. J Lermusiaux. Adaptive modeling, adaptive data assimilation and adaptive sampling. *Physica D: Nonlinear Phenomena*, 230(1):172–196, 2007.

[6] Geospatial big data: Challenges and opportunities. *Big Data Research*, 2(2):74–81, Feb 2015.

[7] http://ngwww.ucar.edu/whatisncarg.html.

[8] Advanced lagrangian predictions for hazards assessments (nsf-alpha): https://goo.gl/b2alky/. *MSEAS-MIT.*

[9] Precision ocean interrogation, navigation, and timing (point) posydon-mit-bbn: http://mseas.mit.edu/research/posydon-point/. *MSEAS-MIT.*

[10] Northern arabian sea circulation - autonomous research: Optimal planning systems (nascar-ops): http://mseas.mit.edu/research/nascar-ops/. *MSEAS-MIT.*

[11] P. F. J. Lermusiaux, P. J. Haley, Jr., S. Jana, A. Gupta, C. S. Kulkarni, C. Mirabito, W. H. Ali, D. N. Subramani, A. Dutt, J. Lin, A. Shcherbina, C. Lee, and A. Gangopadhyay. Optimal planning and sampling predictions for autonomous and lagrangian platforms and sensors in the northern Arabian Sea. *Oceanography*, 30(2):172–185, June 2017. Special issue on Autonomous and Lagrangian Platforms and Sensors (ALPS).

[12] Mseas sea exercises. vorticity: https://goo.gl/2u8cuk, backward ftle: https://goo.gl/qhskbw, standard deviation of sound speed: https://goo.gl/u8ujof, temperature: https://goo.gl/tb6cqa.

Chapter 4

Map Design and Implementation

The need for interactive maps that characterize ocean fields and their uncertainties was established in the previous chapter. This chapter discusses the engineering process adopted while designing these maps and describes, in details, the steps of the process from software selection to styling methods.

The process of selecting the appropriate software program and libraries to design the maps consists of identifying the desired features and capabilities, evaluating a list of options, and selection. Here, we discuss each step.

4.1 The Wishlist

The wishlist is a list of features and capabilities the map and the corresponding software library are expected to possess. In our project, the desired features are:

a. **Lightweight maps**: The web maps are expected to provide a fast user experience and handle many users at the same time without affecting their performance rate.

b. **Browser compatibility**: The web maps and the coding software are expected to be compatible across different browsers. Main browsers to be covered are Chrome, Internet Explorer, Firefox, Opera and Safari.

c. **Mobile device friendliness**: Having a mobile-friendly web map is of critical importance as smartphone traffic is rising to exceed desktop traffic. The product is also expected to run on different operating systems for mobile devices.

d. **Multidimensional visualization capabilities**: In order to match the nature of the ocean fields and uncertainties and their change with space and time, the used software library should support multidimensional capabilities.

e. **Open source and mature library**: It is important to use a software library that is open-source and that has extensive API documentation. The ability to reach out to library developers and a plethora of supporting plugins are fringe benefits.

f. **Modern visuals**: As discussed in good data visualization requirements, it is important that the used library supports modern-looking graphics.

g. **Minimized disruption to existing processes and workflow**: Although this seems to be a local concern, it is crucial to select a design process that causes minimal disturbance to the current data cycle in the MSEAS group. The data fields to be visualized are big data sets that are generated in the back end in a certain fashion. Building upon this fashion and expanding into the web requires certain capabilities discussed in the next section.

4.2 The Options

Similar to any engineering process, after identifying the needs and constraints of the problem, developing possible solutions and iterating over their end use are necessary to build a prototype. As a team in MSEAS, we considered and discussed several options for the flow of the data cycle. These are summarized below.

4.2.1 Option 1

MSEAS traditional data generation practice + a JavaScript mapping library. This involves:

1. Performing numerical computation locally in the back end: Performance enhancing techniques such as optimized scripts and parallel analysis frameworks are considered.
2. Generating georeferenced data files of a certain format compatible with the used library: these are files that list the scalar quantities of an ocean scalar field at points in space (intersection of a latitude and longitude lines) and time, or the scalar quantities of the two components of an ocean vector field (e.g. barotropic and baroclinic velocities of the velocity vector field).
3. Saving the data files in a web directory (such as the MSEAS run PE directories)
4. Visualizing the data on web/mobile devices by writing a Javascript code that utilize the Leaflet mapping library and the d3.js data handling library.

4.2.2 Option 2

"On-the-fly" cloud computation + a JavaScript mapping library. This involves:

1. Moving the raw data to a server (or to the cloud)
2. Performing numerical computations on the cloud in response to a certain request fired in a web/mobile device using (1) "xarray", a Python package that uses powerful N-dimensional variants of the pandas data structures [1], and (2) "Dask", a parallel computing library for analytics [2].
3. Saving the output in georeferenced data files
4. Visualizing the data on web/mobile devices by writing a Javascript code

4.2.3 Option 3

"On-the-fly" cloud computation with "Dash". This involves:

1. Moving the raw data to a server (or to the cloud)

2. Performing numerical computations on the cloud in response to a certain request fired in a web/mobile device using "xarray" and "Dask"

3. Using "Dash", a Python web-based interface framework [3], to serve interactively without Javascript

4.2.4 Option 4

"OPenDAP" and "LAS". This *advanced* option involves:

1. Writing model output in a form compliant with "OPenDAP", a protocol, formerly used for distributed oceanographic data systems, for the retrieval, sampling, analyzing and displaying of datasets [4].

2. Installing a live access server, "LAS", on MSEAS.

3. Serving the output using "PyFerret", an interactive computer visualization designed to meet the needs of oceanographers and meteorologists analyzing complex gridded data sets [5].

Assessing the different options focused on respecting the workflow constraints and achieving the wishlist in a quick time over the summer. Although options such as the fourth seem to be highly attractive for oceanographic applications, the first option showed the most promise with a lot of modern software within the limitations of the group and without disrupting the data generation phase.

Therefore, option 1 is selected.

4.3 The New Interactive Visualization Code

Our new code that generates the interactive maps is written in JavaScript language, embedded in an HTML environment and styled with CSS language. These three components are selected because they are simply the three core technologies of the World Wide Web, and they support the necessities of an effective web experience. The code is written using a text editor, Sublime Text.

The map design process mainly makes use of two JavaScript libraries. These are:

1. **Leaflet**: This is the most popular mapping library today. It is an open-source, very well-documented JavaScript library that supports a wide range of interactivity options. The library is lightweight, flexible, and its plugins are compatible with a variety of data file formats. Leaflet handles the creation of the map with its features and capabilities such as zooming and panning [6]. It also takes control of the ocean field visualization and all the other components the user interacts with on the screen.

2. **d3.js**: This is a data-driven document JavaScript library that helps read data files and handles events in a user desired format [7].

4.4 The Map

After carefully selecting the mapping tools, several versions of the ocean data map were executed. The current version, that supports all the wishlist capabilities, is shown in Figure 4-1

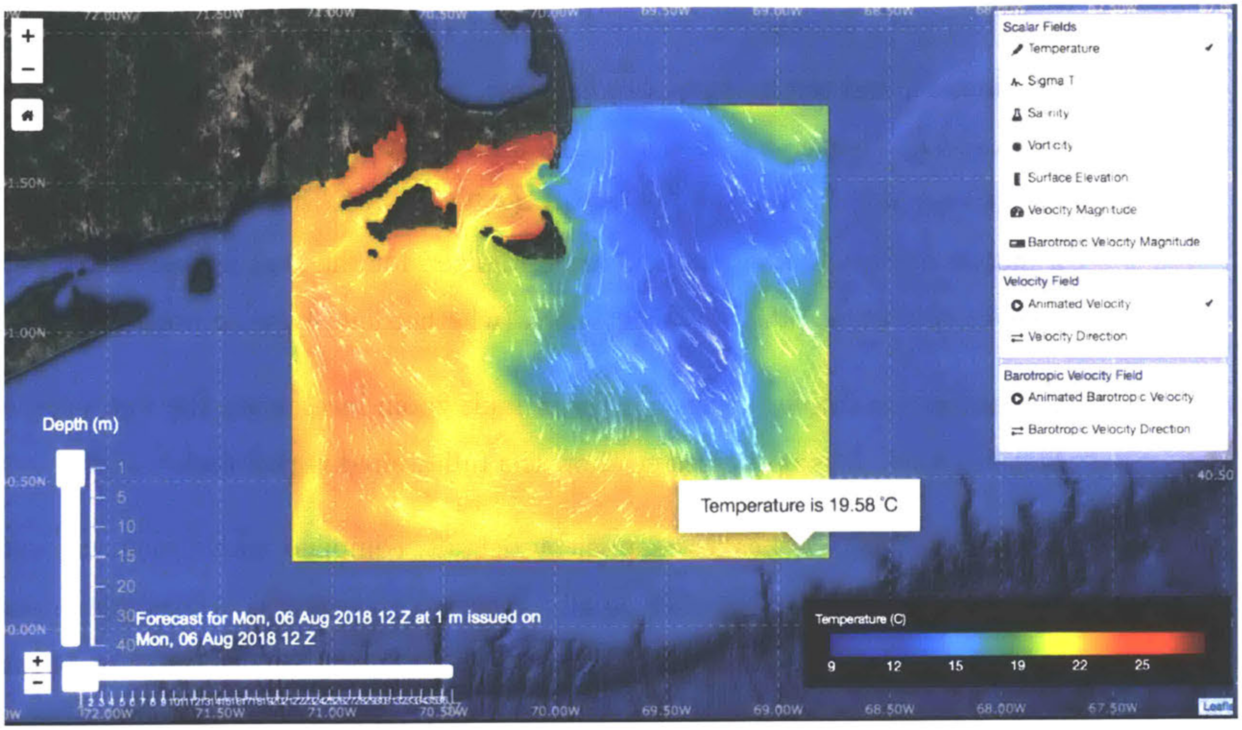

Figure 4-1: The Map View: a schematic of a generated map that shows a temperature field and a snapshot of the animated velocity field around the Martha's Vineyard and Nantucket's coastal region; part of the NSF-ALPHA MSEAS sea exercise issued on August 6^{th}, 2018

The map is made up of a number of components. These components are summarized below.

4.4.1 The Map Variable

Creating a simple blank map in Leaflet starts with hosting an html page in the text editor, calling the leaflet CSS stylesheets, calling the Leaflet script file, creating a <div> element that holds the map, specifying a height style for the map div, and writing a short script that creates the map variable.

The map variable is created using the function "*L.map*" that specifies options such as:

1. **Home center**: this is a an array of two numbers, the latitude and longitude of the center of the page. In our project, the "*home_lat*" and "*home_lon*" vari-

ables are to be specified in a universal input file depending on the sea exercise, the domain, and the browser. For example, in the full domain of NSF-ALPHA sea exercise, "*home_lat*" is set to 40.9 on a desktop device and 40.8 on a mobile device, and "*home_lon*" is set to -69.7 on a desktop device and -70.1 on a mobile device. These numbers are optimized for the best appearance on all devices and across different orientations (whether landscape or portrait).

2. **Home zoom**: "*home_zoom*" is the default zoom level when the web page is first accessed. It is optimized to show the full desired region under study.

3. **Zoom fraction**: A Leaflet map is, by default, equipped with "zoom in" and "zoom out" buttons. One click on any of these two buttons corresponds to one zoom level. Leaflet supports 18 zoom levels at maximum. In order to better control the view of the map, the zoom fraction is set by assigning a fraction of 0.1 to the "*zoom_delta*" variable.

4.4.2 Baselayer Map

The baselayer map is a tiled layer imported from an online web server, such as Google Maps, Open Street Maps or Map Box. In our project, the base layer is a Google satellite image. It was selected because it shows some definition in the oceanic regions such as lined shelves and ridges. The function "*L.tilelayer()*" is used to assign this base layer using a URL address that usually ends with: z/x/y, which is a template that Leaflet uses to find tiles at the correct zoom, x, and y coordinates [8]. The function "*add.To(map)*" is used to add the base layer to the <div> holder created when the map variable is initialized.

4.4.3 Data Layers

The data overlaid on the base layer represents the heart of the new code and the bottleneck of the mapping process. Examples of data layers, from the NSF-ALPHA sea exercise are shown in Figure 4-2 and others from the POSYDON-POINT sea exercise are shown in Figure 4-3. This step takes care of reading the geospatial data files, analyzing their content, transforming the content into scalar color maps or vector fields, and visualizing the data in an efficient, fast way. In a broader perspective, iterating through different options of the data layers represents the bottleneck of the project because of its importance in telling the story of the data.

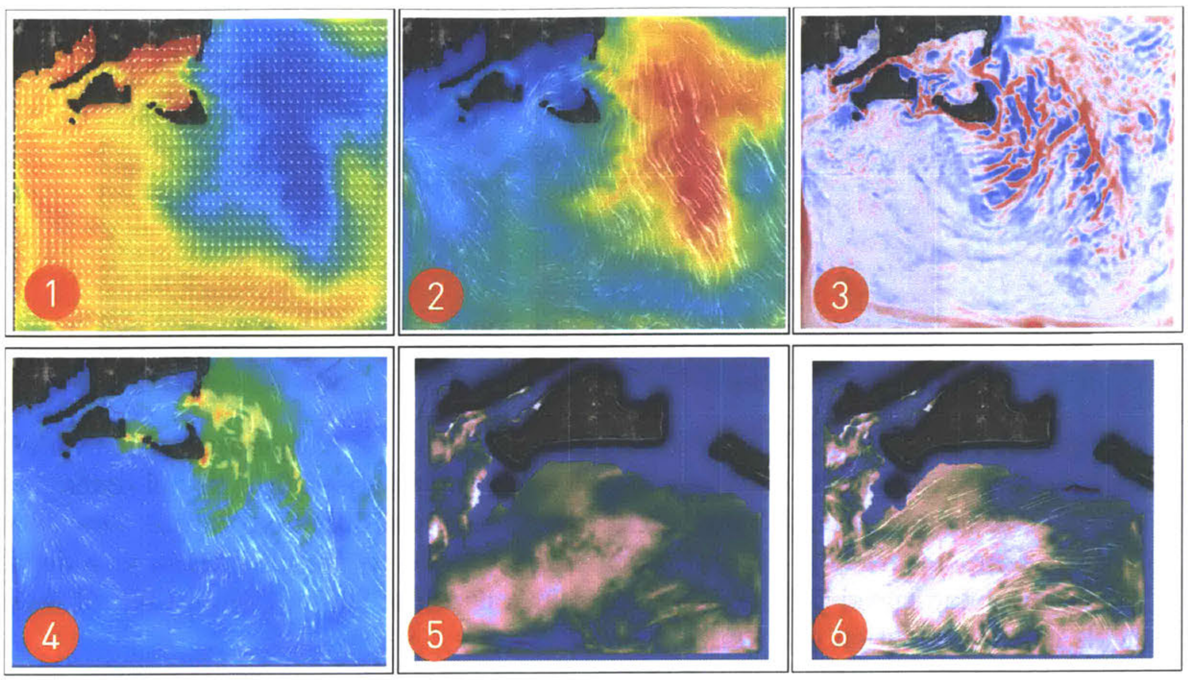

Figure 4-2: 2018 NSF-ALPHA Data Layer Snapshots - (**1**: Temperature field overlaid with velocity direction field in full domain at 0 m, **2**: salinity field overlaid with animated velocity in full domain at 0 m, **3**: vorticity field in full domain at 0 m, **4**: velocity vector field (magnitude and direction) in full domain at 0 m, **5**: standard deviation field of the seawater density in zoomed-in domain at a depth of 20 m, **6**: standard deviation field of temperature overlaid with mean animated velocity field in zoomed-in domain at a depth of 20 m). Note that the fields of 1,2,3, and 4 have a 600 m resolution, while those of 5 and 6 have a 200 m resolution

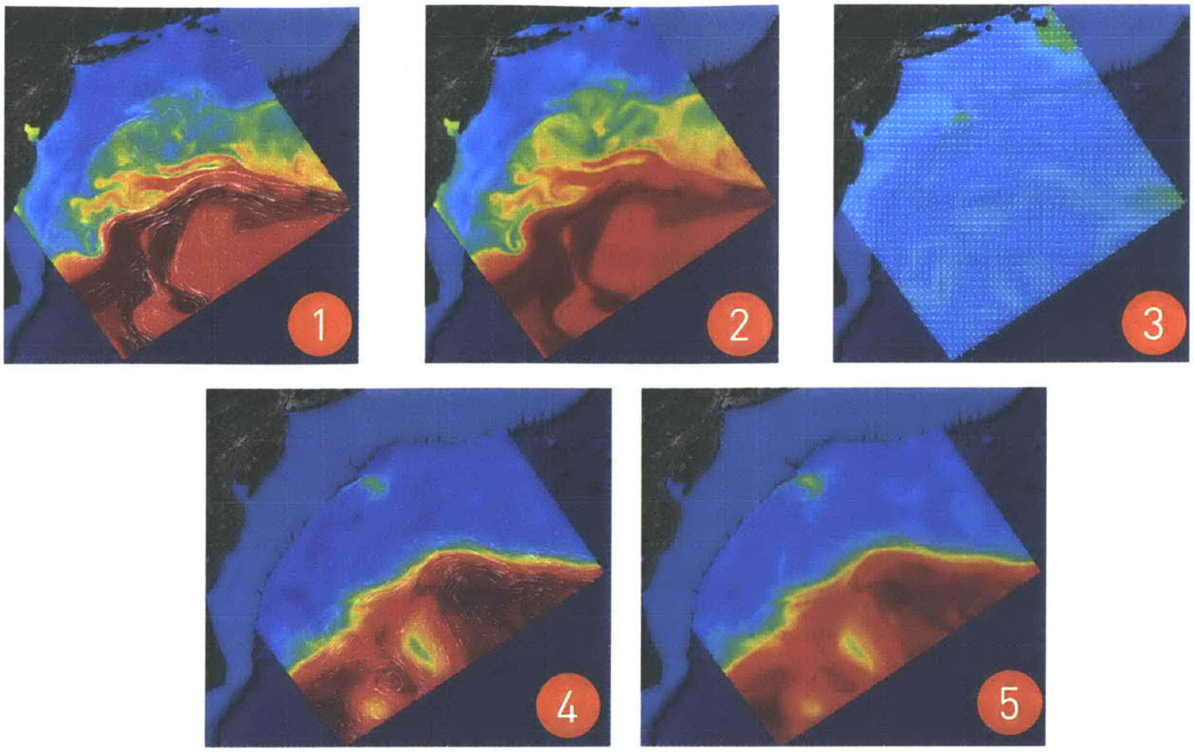

Figure 4-3: POSYDON-POINT Data Layer Snapshots - (**1**: temperature field overlaid with animated velocity in full domain at 0 m, **2**: sound speed field in full domain at 0 m, **3**: barotropic velocity vector field (magnitude and direction) in full domain at 0 m, **4**: temperature field overlaid with animated velocity in full domain at a depth of 500 m, sound speed field in full domain at a depth of 500 m). Note that all these fields have a resolution of 3 km.

The following steps are executed to produce these data layers:

1. **Data File Generation**: The PE model numerically computes the fields. Big data sets are stored in either "mat" files (MATLAB formatted structures) or "NetCDF" files. A MATLAB script loads these data files and writes them in ASCII format. ASCII is a character encoding standard for electronic communication [9]. In the context of our maps, a sample ASCII file format is shown in Figure 4-4. This example is a salinity field at a depth of 20 m for an NSF-ALPHA sea exercise with a resolution of 600 m. In this example, 445 × 281 data points are on the grid. The rectangular grid is bound by a latitude line of 40.22 and a longitude line of -71.18. The horizontal or vertical difference between two consecutive points correspond to 0.0054 degrees. Salinity data is

listed as text, in which a value of -9999.00 corresponds to a no-data point in space (e.g. a point on land or a a point outside the domain).

```
ncols 445
nrows 281
xllcorner -71.18259
yllcorner 40.22916
cellsize 0.00541
NODATA_value -9999.00000
-9999.00000 -9999.00000 -9999.00000 -9999.00000 -9999.00000 -9999.00000 -9999.00000 -9999.00000 -9999.00000 -9999.00000 -9999.00000 -9999.00000
-9999.00000 -9999.00000 -9999.00000 -9999.00000 -9999.00000 -9999.00000 -9999.00000 -9999.00000 -9999.00000 -9999.00000 -9999.00000 -9999.00000
-9999.00000 -9999.00000 -9999.00000 -9999.00000 -9999.00000 -9999.00000 -9999.00000 -9999.00000 -9999.00000 -9999.00000 -9999.00000 -9999.00000
-9999.00000 -9999.00000 -9999.00000 -9999.00000 -9999.00000 -9999.00000 -9999.00000 -9999.00000 -9999.00000 -9999.00000 -9999.00000 -9999.00000
-9999.00000 -9999.00000 -9999.00000 -9999.00000 -9999.00000 -9999.00000 -9999.00000 -9999.00000 -9999.00000 -9999.00000 -9999.00000 -9999.00000
-9999.00000 -9999.00000 -9999.00000 -9999.00000 -9999.00000 -9999.00000 -9999.00000 -9999.00000 -9999.00000 -9999.00000 -9999.00000 -9999.00000
-9999.00000 -9999.00000 -9999.00000 -9999.00000 -9999.00000 -9999.00000 -9999.00000 -9999.00000 -9999.00000 -9999.00000 -9999.00000 -9999.00000
-9999.00000 -9999.00000 -9999.00000 -9999.00000 -9999.00000 -9999.00000 -9999.00000 -9999.00000 -9999.00000 -9999.00000 -9999.00000 -9999.00000
-9999.00000 -9999.00000 -9999.00000 -9999.00000 -9999.00000 -9999.00000 -9999.00000 -9999.00000 -9999.00000 -9999.00000 -9999.00000 -9999.00000
-9999.00000 -9999.00000 -9999.00000 -9999.00000 -9999.00000 -9999.00000 -9999.00000 -9999.00000 -9999.00000 -9999.00000 -9999.00000 -9999.00000
-9999.00000 -9999.00000 -9999.00000 -9999.00000 -9999.00000 -9999.00000 -9999.00000 -9999.00000 -9999.00000 -9999.00000 -9999.00000 -9999.00000
-9999.00000 -9999.00000 -9999.00000 -9999.00000 -9999.00000 -9999.00000 -9999.00000 -9999.00000 -9999.00000 -9999.00000 -9999.00000 -9999.00000
-9999.00000 -9999.00000 -9999.00000 -9999.00000 -9999.00000 -9999.00000 -9999.00000 -9999.00000 -9999.00000 -9999.00000 -9999.00000 -9999.00000
-9999.00000 -9999.00000 -9999.00000 -9999.00000 -9999.00000 -9999.00000 -9999.00000 -9999.00000 -9999.00000 -9999.00000 -9999.00000 -9999.00000
-9999.00000 -9999.00000 -9999.00000 -9999.00000 -9999.00000 -9999.00000 -9999.00000 -9999.00000 -9999.00000 -9999.00000 -9999.00000 -9999.00000
-9999.00000 -9999.00000 -9999.00000 -9999.00000 -9999.00000 -9999.00000 -9999.00000 -9999.00000 -9999.00000 -9999.00000 -9999.00000 -9999.00000
-9999.00000 -9999.00000 -9999.00000 -9999.00000 -9999.00000 -9999.00000 -9999.00000 -9999.00000 -9999.00000 -9999.00000 -9999.00000 -9999.00000
-9999.00000 -9999.00000 -9999.00000 -9999.00000 -9999.00000 -9999.00000 -9999.00000 -9999.00000 -9999.00000 -9999.00000 -9999.00000 -9999.00000
-9999.00000 -9999.00000 -9999.00000 -9999.00000 -9999.00000 -9999.00000 -9999.00000 -9999.00000 -9999.00000 -9999.00000 -9999.00000 -9999.00000
-9999.00000 -9999.00000 -9999.00000 -9999.00000 -9999.00000 -9999.00000 -9999.00000 -9999.00000 -9999.00000 -9999.00000 -9999.00000 -9999.00000
-9999.00000 32.34841 32.30341 32.37103 32.40216 32.50221 32.65450 32.62774 32.65852 32.71160 32.86946 32.88129 32.87412 32.88707 32.81543
32.79451 32.94562 33.08875 33.07708 32.99919 32.80142 32.64847 32.64547 32.68692 32.76182 32.83402 32.87938 32.79045 32.63521 32.63199 32.77874
32.87580 32.82902 32.71957 32.63068 32.56963 32.56455 32.59431 32.65414 32.70209 32.67886 32.65970 32.63589 32.63896 32.64459 32.65311 32.66349
32.67373 32.67281 32.66687 32.65985 32.65433 32.65576 32.65802 32.65479 32.64879 32.64417 32.63291 32.61862 32.60899 32.58325 32.55859 32.53672
32.51886 32.51687 32.54268 32.52871 32.49290 32.47214 32.44766 32.43000 32.41159 32.40906 32.41549 32.41548 32.40601 32.38995 32.37644 32.36876
32.36640 32.36292 32.35785 32.35190 32.34401 32.33796 32.32985 32.32354 32.31782 32.31452 32.31299 32.31073 32.30930 32.30501 32.30415 32.30371
32.30524 32.30215 32.30168 32.30024 32.29819 32.29518 32.29079 32.28639 32.28333 32.28403 32.28572 32.28735 32.28787 32.28569 32.28723 32.29157
32.29334 32.29411 32.29767 32.30140 32.30489 32.30806 32.31044 32.31207 32.31391 32.31640 32.31984 32.32602 32.33254 32.33973 32.34690 32.35410
32.36092 32.36697 32.37251 32.37866 32.38481 32.39165 32.39905 32.40815 32.41762 32.42706 32.43657 32.44425 32.45050 32.45538 32.45997 32.46458
32.46928 32.47434 32.48076 32.48864 32.49686 32.50439 32.51120 32.51731 32.52314 32.52642 32.52557 32.51807 32.50634 32.49794 32.49539 32.50060
32.51121 32.52262 32.53459 32.54709 32.55837 32.56932 32.57657 32.58213 32.58573 32.58808 32.59185 32.59734 32.60621 32.61592 32.62453 32.63162
32.63429 32.63697 32.63907 32.64021 32.64074 32.64005 32.63855 32.63490 32.63372 32.63225 32.63087 32.62953 32.62905 32.62682 32.62337 32.61695
32.61020 32.60375 32.59635 32.58732 32.57689 32.56417 32.55235 32.54424 32.54218 32.55555 32.57650 32.60002 32.62123 32.63164
-9999.00000 -9999.00000 -9999.00000 -9999.00000 -9999.00000 -9999.00000 -9999.00000 -9999.00000 -9999.00000 -9999.00000 -9999.00000 -9999.00000
-9999.00000 -9999.00000 -9999.00000 -9999.00000 -9999.00000 -9999.00000 -9999.00000 -9999.00000 -9999.00000 -9999.00000 -9999.00000 -9999.00000
-9999.00000 -9999.00000 -9999.00000 -9999.00000 -9999.00000 -9999.00000 -9999.00000 -9999.00000 -9999.00000 -9999.00000 -9999.00000 -9999.00000
-9999.00000 -9999.00000 -9999.00000 -9999.00000 -9999.00000 -9999.00000 -9999.00000 -9999.00000 -9999.00000 -9999.00000 -9999.00000 -9999.00000
```

Figure 4-4: Sample ASCII File Format (taken from a salinity field)

2. **Data File Placement**: The generated ASCII files are saved in the PE directory in a folder named "Data". Note that within a sea exercise and domain, each file correspond to a certain depth and a certain time of modeling. A universal naming standard has to be created in order to accommodate this information. Figure 4-4 is taken from a file called: "S0020m_Hz600m001_009.asc" where "S" means salinity, "0020m" means the field is at a depth of 20 m below the surface, "Hz600m001" is a project ID conventionally used in MSEAS, and "009" means the ninth time since the issue of the exercise.

3. **Data File Reading**: The code reads the data from the ASCII file using a d3.js operator called "*d3.text()*".

4. **Data Rendering**: Scalar field colormaps are plotted using a Leaflet operator called "*L.CanvasLayer.Field*". The operator hosts a number of options such as opacity control, cursor availability within the field, and color scale support. A

screenshot of the code that renders a sample salinity profile is shown in Figure 4-5

```
//Salinity

d3.text(salt_file_name, function (asc) {
    var sal = L.ScalarField.fromASCIIGrid(asc);

    salrange = colorbarKeyVal[salt_color_string];

    salscale = chroma.scale(['#00008F', '#00009F', '#0000AF', '#0000BF', '#0000CF', '#0000DF', '#0000EF', '#0000FF', '#0010FF'
        , '#0020FF', '#0030FF', '#0040FF', '#0050FF', '#0060FF', '#0070FF', '#0080FF', '#008FFF', '#009FFF', '#00AFFF', '
        #00BFFF', '#00CFFF', '#00DFFF', '#00EFFF', '#00FFFF', '#10FFEF', '#20FFDF', '#30FFCF', '#40FFBF', '#50FFAF', '#60FF9F'
        , '#70FF8F', '#80FF80', '#8FFF70', '#9FFF60', '#AFFF50', '#BFFF40', '#CFFF30', '#DFFF20', '#EFFF10', '#FFFF00', '
        #FFEF00', '#FFDF00', '#FFCF00', '#FFBF00', '#FFAF00', '#FF9F00', '#FF8F00', '#FF8000', '#FF7000', '#FF6000', '#FF5000'
        , '#FF4000', '#FF3000', '#FF2000', '#FF1000', '#FF0000', '#EF0000', '#DF0000', '#CF0000', '#BF0000', '#AF0000', '
        #9F0000', '#8F0000', '#800000']).domain(salrange);

    sallayer = L.canvasLayer.scalarField(sal, {
        interpolate: true,
        color: salscale,
        mouseMoveCursor: null
    }).setOpacity(0.7);
    }
});
```

Figure 4-5: Data Rendering of a Scalar Field

On the other hand, vector animated fields are generated using the operator "*L.CanvasLayer.vectorFieldanim*". Plotting a vector field requires two data files, one for the horizontal component and another for the vertical component of the field. The function then takes care of calculating the magnitude, direction, and animating the field.

5. **Popup Function**: A popup function is written to allow the user to interact with the data field by clicking on a certain point in space (latitude, longitude, depth) and time. An example of the function and output is shown in Figure 4-6.

```
//Salinity Layer Popup

sallayer.on('click', function (e) {
    if (e.value !== null) {
        let S = e.value.toFixed(2);
        let html = `<span class="popupText">Salinity is ${S} psu</span>`;
        let popup = L.popup().setLatLng(e.latlng).setContent(html).openOn(map);
    }
});
```

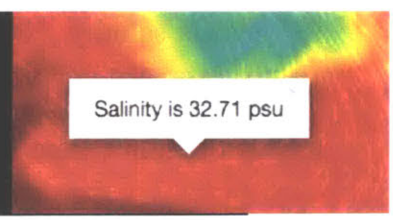

Figure 4-6: Popup Function Example (salinity field)

6. **Color Scale and Color Bar**: The color scale is read using a JavaScript library called Chroma.js. As shown in the salinity example of Figure 4-5, the color scale is inserted as a hex code. MSEAS traditionally uses certain color schemes for

certain ocean fields. A MATLAB function that transforms the RGB matrices used by MSEAS is used to generate the hex codes.

A color bar is then added to the layer. The control function supports options such as a title, number of color steps, number of decimals in the labels, width, height and position, text color and background color. An example of the function and its output is shown in Figure 4-7. Special attention is given to color bars of web maps viewed on mobile devices.

```
var salstep = (1 / nlabels) * (salrange[1] - salrange[0]);
salbar = new L.control.colorBar(salscale, salrange, {
    title: 'Salinity (psu)',
    units: 'psu',
    steps: 64,
    decimals: 1,
    width: Math.min(350, screen.width / 3),
    height: Math.min(20, screen.height / 12),
    position: 'bottomright',
    background: backgroundcolor,
    textColor: 'white',
    labels: range(salrange[0], salrange[1], salstep),
    labelFontSize: 13
});
```

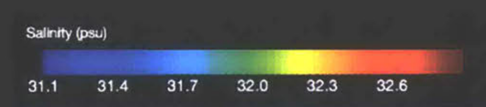

Figure 4-7: Salinity Colorbar Example

4.4.4 Control Panel

The control panel is the vehicle through which the user interacts with the map and the different ocean data fields. It is the sphere in which the user has the most control. It is generated using a Leaflet control function called: "*L.control.panelLayers*". In ocean physics maps, the control panel categorizes the data in regards to their scalar or vector nature. In ocean uncertainty maps, the control panel divides the fields between mean and standard deviation fields.

The control panel layers are coded with checkboxes, giving the user the option to select more than one layer at a time. Selecting or deselecting a layer modifies two checkbox event listeners called "*overlayadd*" and "*overlayremove*". Listening to these events, functions are written to add map components corresponding to the shown ocean field. For example, if the salinity layer is selected, the map listens to "*sallayer.on*" under "*overlayadd*" and automatically activates the salinity popup function and adds the salinity color bar. Example control panels are shown in Figure 4-8.

Figure 4-8: Example Control Panels - 1: an ocean physics map, 2: an ocean uncertainty map

4.4.5 Sliders

Time and depth sliders are <div> elements that are coded to respond to users' requests of data that vary spatiotemporally. These two components give the map its 4-D capability. They are coded using a JavaScript range slider package called "noUiSlider". They are lightweight and properly function on all devices.

- **Depth Slider**: Tapping on a certain location along the slider updates an event listener called "*depthSlider.noUiSlider.on(set)*". The updated value is coded to change the name of the file read by "*d3.text()*", thereby generating the new ocean data field. Pips are also added to the slider.

- **Time Slider**: The time slider works in a similar fashion. Changing the location of the handle updates the "set" event listener and subsequently updates the name of the file to be read by "*d3.text()*". Since some of the sea exercise maps showcase 40 times on one slider, two <div> buttons are also added. Clicking on the plus or minus buttons to the left of the time slider, respectively increment or decrement the time by one step. The "click" event listener of the button, and the "set" event listener of the time slider are synchronized.

A screenshot of each of the sliders and the time step button are shown in Figure 4-9.

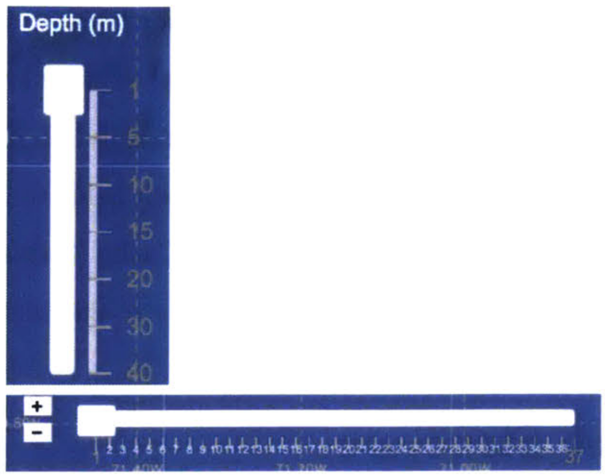

Figure 4-9: Depth and Time Range Sliders

4.4.6 Other elements

The map webpages host a number of other elements, some of which are:

- **Home Button**: This is a <div> button that, once clicked, returns the map to the user-specified home zoom level.

- **Download Button**: This is a <div> button that allows the user to save the current snapshot of the map and its components as a "png" image on their device.

- **Time Stamp**: Below the ocean field, a <div> text is added. It matches the text MSEAS use with their images. An example text is: "Forecast for Tue, 07 Aug 2018 4 Z at 1 m issued on Mon, 06 Aug 2018 12 Z". The stamp gives the full date and Zulu time of the demonstrated field in addition to the depth of the field and the issue date of the exercise.

- **Latitude and Longitude Lines**: The latitude-longitude grid in the shown domain is added to the map using a function called "*L.latlngGraticule*". The coordinate lines are updated with the zoom level of the map.

4.4.7 Cache Function

The map design code includes some other functions that are meant to enhance the performance of the map and mainly reduce the latency between the ocean fields. This eventually provides the user with a fast, simple, yet powerful web experience. The slowest step in the data visualization process is naturally loading and rendering the data file. In order to minimize the time it takes ocean fields to appear on screen, the code saves previously loaded layers in the browser Cache (Subramani). The function proves to decrease the loading time of a big data file to 200-300 ms.

4.5 The Web Structure

In the *back end* of every map's URL, there is an index file that contains the Leaflet map code and two folders:

- **"Data"**

  This folder contains:

  1. *Data Files*: these are all the ASCII files necessary to plot ocean fields. The ASCII files follow a standard naming procedure similar to that of the salinity example, previously discussed.
  2. *Input File*: In order to minimize the number of required edits in case a code is to be used for a future project, the code is written in a way that any edit of the input requirement should be done within this JavaScript file. An example of a similar file is shown in Figure 4-10.

```
var temp_lead_string = 'Data/T';
var salt_lead_string = 'Data/S';
var vort_lead_string = 'Data/vorticity';
var height_lead_string = 'Data/Eta';
var uvel_lead_string = 'Data/U';
var vvel_lead_string = 'Data/V';
var ubaro_lead_string = 'Data/Ubaro';
var vbaro_lead_string = 'Data/Vbaro';
var wvel_lead_string = 'Data/W';
var sigt_lead_string = 'Data/SigT';
var available_depths = [1,5,10,15,20,30,40];
var issue_date_str = 'Aug.06,2018 12:00:00 UTC';
var forecast_start = 1.500000;
var start_time = 12.000000;
var time_step = 1.000000;
var startingday = 5.000000;
var monthYear = 'Aug. 2018';
var num_time_steps = 37;
var runid = 'Hz200m001_';

var colorbarKeyVal = {
'T0001m': [19.0910,24.2201],
'S0001m': [31.1361,32.7962],
'VMag0001m': [13.6651,130],
'W0001m': [-0.0362,0.0365],
'vorticity0001m': [-2.0000,2.0000],
'SigT0001m': [21.2483,22.8823],
'C0001m': [1515.2667,1530.1610],
'T0005m': [18.9628,24.2632],
'S0005m': [31.1791,32.7796],
'VMag0005m': [10.3848,140],
'W0005m': [-0.1438,0.1441],
'vorticity0005m': [-2.0000,2.0000],
'SigT0005m': [21.3899,22.9165],
'C0005m': [1514.8826,1529.5395],
'T0010m': [14.9552,23.7792],
'S0010m': [31.2304,32.7618],
'VMag0010m': [10.3408,50],
'W0010m': [-0.1733,0.1739],
'vorticity0010m': [-2.0000,2.0000],
'SigT0010m': [21.5959,23.0599],
'C0010m': [1512.8642,1528.9929],
'T0015m': [15.4284,22.7624],
'S0015m': [31.4057,32.8],
'VMag0015m': [9.8374,30],
'W0015m': [-0.1660,0.1672],
'vorticity0015m': [-2.0000,2.0000],
'SigT0015m': [21.4318,24.4406],
'C0015m': [1503.0936,1526.3803],
'T0020m': [12.0526,22.6447],
'S0020m': [31.5028,32.9277],
'VMag0020m': [9.5423,50],
'W0020m': [-0.1436,0.1450],
'vorticity0020m': [-2.0000,2.0000],
'SigT0020m': [21.4236,24.9549],
'C0020m': [1492.3513,1526.3265],
'T0030m': [10.6143,18.4949],
'S0030m': [31.8101,33.0688],
'VMag0030m': [6.5824,50],
'W0030m': [-0.0610,0.0624],
'vorticity0030m': [-2.0000,2.0000],
'SigT0030m': [23.2383,25.4059],
'C0030m': [1488.2085,1508.8180],
'T0040m': [9.7214,12.0170],
'S0040m': [32.5078,33.1168],
'VMag0040m': [1.7504,33.1616],
'W0040m': [-0.0394,0.0407],
'vorticity0040m': [-2.0000,2.0000],
'SigT0040m': [24.6411,25.5146],
'C0040m': [1487.1841,1495.0451],
'Eta': [-1.0000,1.0000],
'VbaroMag': [11.4760,183.2734],
}
```

Figure 4-10: Input File Parameters

- **"Src"**

  This folder contains two main categories of files, described below:

  1. *Script Files*: These are JavaScript files that contain the necessary information for the libraries, packages and plugins to perform their full functionality. The files needed in the design of our maps are (1) "d3.v4.js" that handles data reading, (2) "leaflet.js" that handles the map creation and function, (3) "leaflet.canvaslayer.field.js" that plots scalar color fields and vector arrow fields, (4) "chroma.js" that manages color manipulations, (5) "easy-button.js" that allows the creation of click buttons on the map, (6) "nouislider.js" that handles the function of the time and depth sliders, (7) "wNumb.js", an accessory of range sliders that manages number formatting, (8) "leaflet-panel-layers.src.js" that creates and operates the control panel, and (9) "leaflet.latlng-graticule.js" that manages the coordinate lines on the map.

  2. *CSS Files*: These are plain-text formatted files that manage the style associated with each library, package, plugin or function. In addition to style sheets of the previous script files, this project uses a font and icon stylesheet provided by Font Awesome. Moreover, styling of <div> elements and their placement relative to the page margins is executed depending on the de-

vice's screen width: devices of a screen width bigger than 800 px use a stylesheet different from the one used by devices whose screen width is 800 px or less (such as mobile devices).

In the *front end*, the web experience provided by MSEAS proves to be more effective and powerful. If the ocean enthusiast of section 3.2.3 is interested in a temperature profile at the surface of the ocean in the POSYDON-POINT region, all they have to do is navigate to the sea exercise's link on the MSEAS page, click "Central Forecast" and the interactive map shows up. These two steps are shown in Figure 4-11.

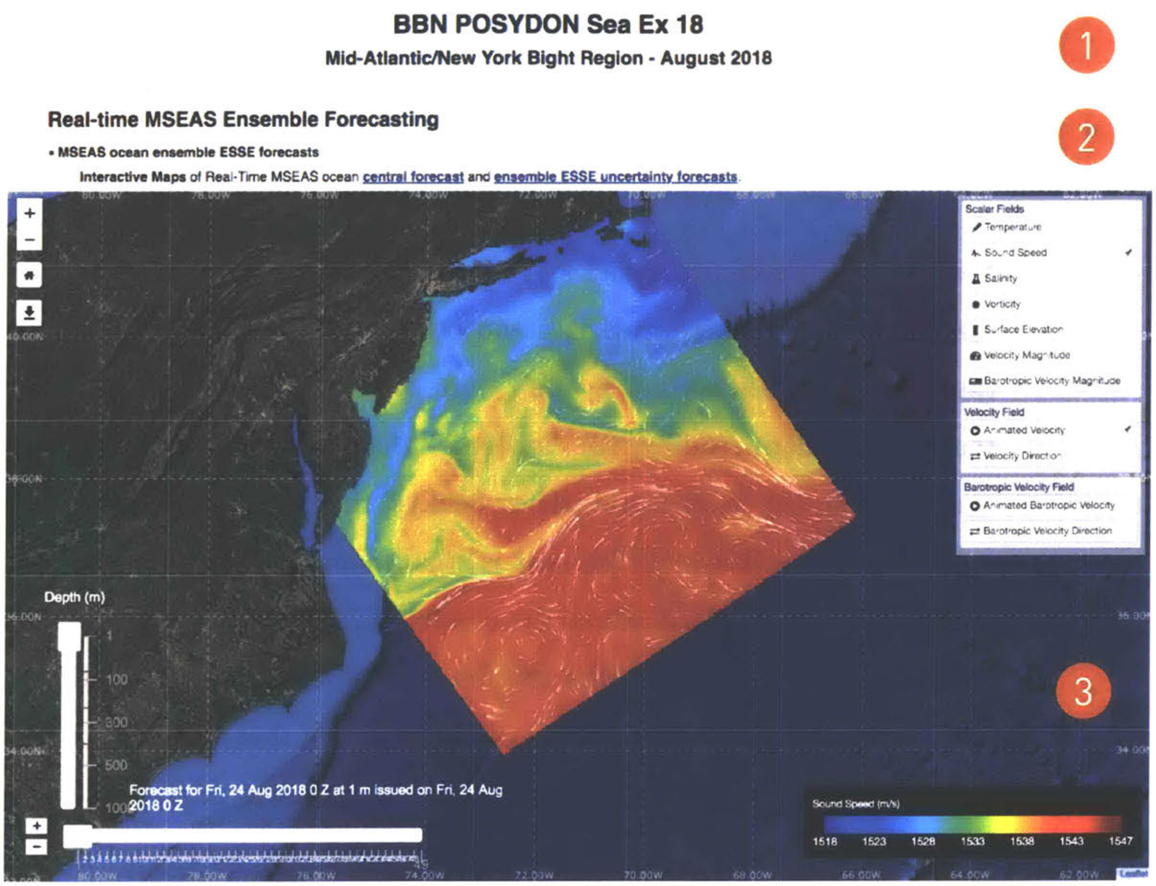

Figure 4-11: New Web *Front End* [10]

4.6 The Mobile Device

Today, it is crucially important to complement the desktop web experience with mobile device access that allows the users to make decisions on the go. Since the selected library shows full browser and device compatibility, the code changes that pertain to mobile devices are limited to styling. A separate styling sheet is created for mobile devices. This sheet manages positions of elements relative to the page margins. In addition, the widths of elements such as color bars, sliders and control panels are assigned as a percentage of the screen width. The control panel is also made collapsible on a mobile device, by default. A screenshot of an ocean map in mobile landscape mode and another in mobile portrait mode are shown in Figure 4-12. Both screenshots are taken on an iPhone 7+.

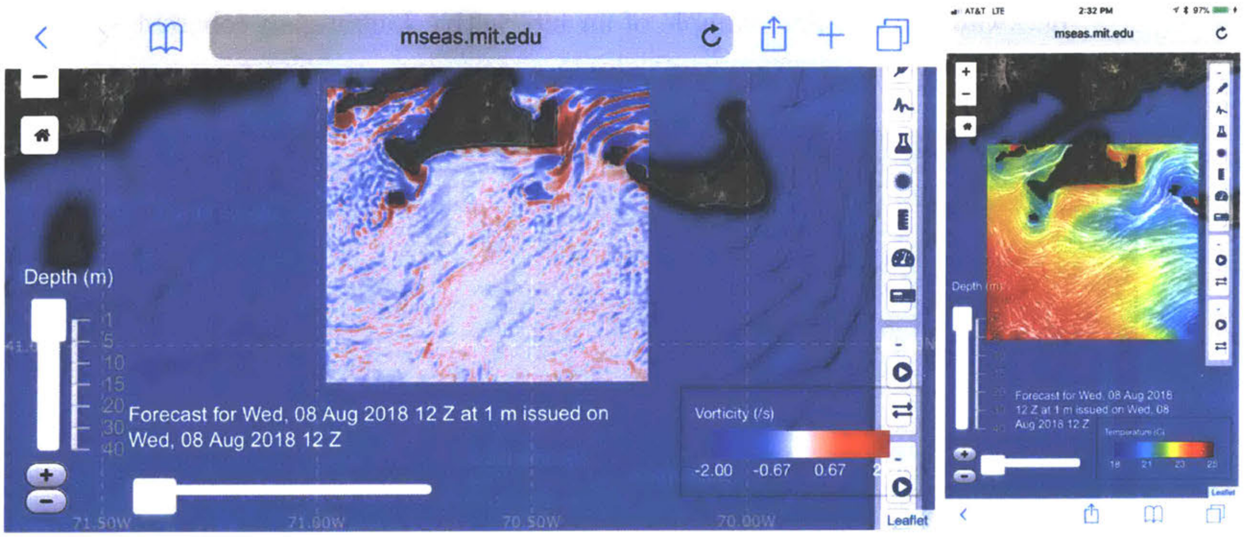

Figure 4-12: Mobile Device Map Views (left: landscape mode, right: portrait mode)

4.7 The Applications

The generated Leaflet maps and their corresponding coding program are flexible and easily extendable to geospatial applications (even non-ocean related ones). Below is a list of four MSEAS applications, the first two of which already utilized these webmaps.

1. **Advanced Lagrangian Predictions for Hazards Assessments (NSF-ALPHA) [11]**

   This project is sponsored by NSF and takes place in the Martha's vineyard and Nantucket coastal region. It implements an integrated theoretical, computational and observational approach to develop, implement and utilize cutting-edge Lagrangian methods with data-driven modeling. It also aims to quantify and predict key transport processes and four-dimensional (3D plus time) structures during regional flow-based hazards in the ocean and atmosphere.

In addition to different ocean physics fields and uncertainties at 600 m and 200 m resolution in full and zoomed in domains, NSF-ALPHA maps of Lagrangian Coherent Structures are created to showcase the scalar fields of the forward and backward FTLE. An example of an interactive Lagrangian coherent structure 6 hour FTLE map is shown in Figure 4-13.

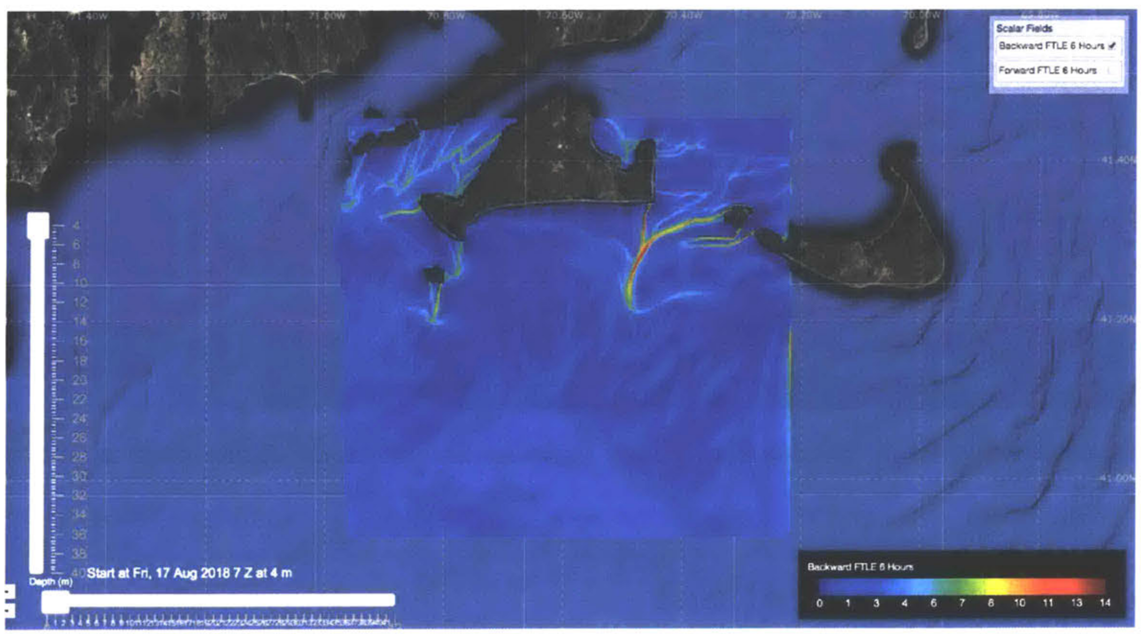

Figure 4-13: NSF-ALPHA LCS 6 hour Backward FTLE Map

2. **Precision Ocean Interrogation, Navigation, and Timing (POINT): POSYDON-MIT-BBN) [12]**

   This project is sponsored by DARPA and takes place in the Bight of New York in the mid-Atlantic. It aims to develop a Global Positioning System (GPS) for underwater assets. In order to achieve that purpose, it applies ocean modeling, data assimilation and uncertainty quantification for the estimation of sound speed variability and applies MSEAS schemes for optimal placement and path planning with varied assets and acoustic source platforms. An example of sound speed maps generated in the POSYDON area is shown in Figure 4-14.

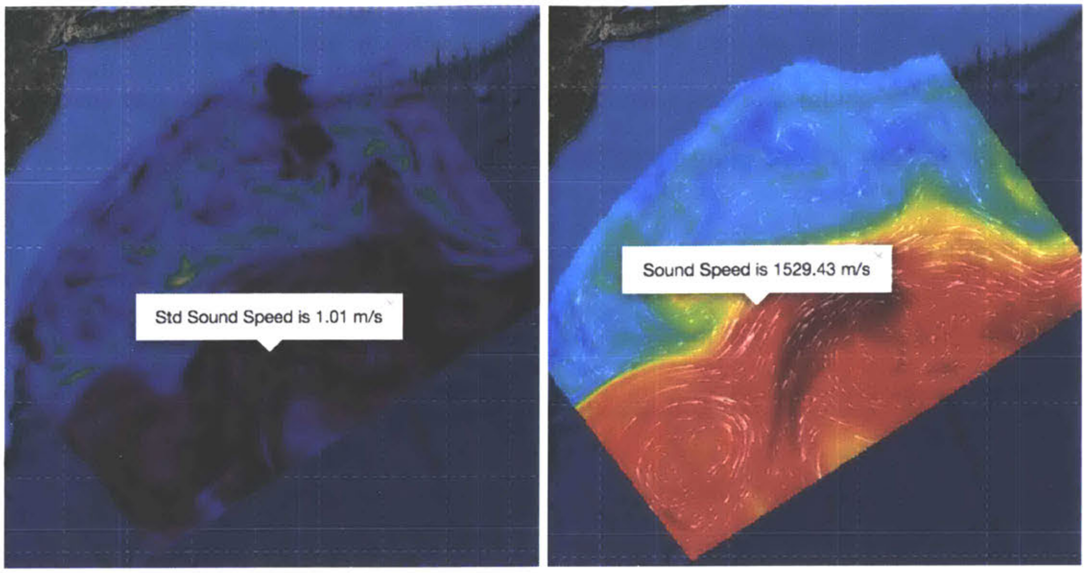

Figure 4-14: POSYDON-POINT Sound Speed Field Maps

3. **Coastal Ocean Sensing and Forecasting for Fisheries Management: Practical Systems for India** [13]

   This project is sponsored by MIT Tata Center and it takes place in the North Bengal and the Arabian Sea. It applies modeling methods and develops ocean physical and biogeochemical forecasting products that provide fisheries with technical aide and more sustainable management tools.

4. **Long-duration Environmentally-adaptive Autonomous Rigorous Naval Systems (LEARNS) [14]**

   This application is sponsored by the Science of Autonomy Program - Office of Naval Research. It aims to develop and apply new theory, algorithms and computational systems for the sustained coordinated operation of multiple collaborative autonomous vehicles over long time durations in realistic multi-scale nonlinear ocean settings.

4.8 The Demo

The power of interactive maps is mainly demonstrated in live online maps. Since it is not possible to show all the capabilities in a written text, what follows are three links for MSEAS ocean maps. (*note* that in case the links expire, you are encouraged to send the author an email and ask for new links).

1. Ocean Physics:
    - NSF-ALPHA 600 m resolution domain: https://bit.ly/2wTwD91
    - POSYDON-POINT 3 km resolution domain: https://bit.ly/2NXpCLV
2. Ocean Uncertainties: https://bit.ly/2MU6Rw9

Bibliography

[1] Stephan Hoyer and Joseph J. Hamman. xarray: N-d labeled arrays and datasets in python. *Journal of Open Research Software*, 5, May 2017.

[2] http://dask.pydata.org Dask: Scalable analytics in Python.

[3] Dash. Modern visualization for the data era - plotly, https://plot.ly/products/dash/. *Dash by Plotly.*

[4] OPENDAP. https://www.opendap.org/pdf/dff.pdf.

[5] PyFerret. Pyferret scientific computing, https://scicomp.ethz.ch/wiki/pyferret.

[6] Leaflet. https://leafletjs.com.

[7] Mike Bostock. Data-driven documents: https://d3js.org/.

[8] MaptimeBoston. Leaflet, https://maptimeboston.github.io/leaflet-intro/.

[9] ASCII. Wikipedia,https://en.wikipedia.org/wiki/ascii. Sep 2018.

[10] Multidisciplinary Simulation Estimation and MIT Assimilation Systems MSEAS. http://mseas.mit.edu/.

[11] Advanced lagrangian predictions for hazards assessments (nsf-alpha): https://goo.gl/b2alky/. *MSEAS-MIT.*

[12] Precision ocean interrogation, navigation, and timing (point) posydon-mit-bbn: http://mseas.mit.edu/research/posydon-point/. *MSEAS-MIT.*

[13] Coastal ocean sensing and forecasting for fisheries management: Practical systems for india: http://mseas.mit.edu/research/tataproject/. *MSEAS-MIT.*

[14] Long-duration environmentally-adaptive autonomous rigorous naval systems (learns): http://mseas.mit.edu/research/learns/. *MSEAS-MIT.*

Chapter 5

Conclusion and Future Work

This thesis starts with the realization of the significance of ocean dynamics data and ends in an interactive robust product that gives the user access to web maps on any device or browser. This chapter concludes the thesis and recommends some enhancements on the new interactive visualization code, maps, and applications.

5.1 Conclusion

The importance of ocean dynamics models and 4-D visualization stems from the profound impact of oceans on the life on Earth. MSEAS utilizes their PE data-assimilative modeling system that forecasts and analyzes fields and uncertainties of a number of prognostic and diagnostic variables. Our new JavaScript code, with the aid of Leaflet and d3.js libraries, generates interactive maps that demonstrate these variables. These maps feature color maps of scalar ocean fields and arrow maps of vector fields. In addition, they host time and depth control sliders, color legends, date stamps and zooming and panning control. The significance of these maps lies in the web experience they offer the user. The user is given the venue to recognize patterns in certain ocean fields and make conclusions, even technical decisions regarding their application. The MSEAS maps eradicate the need for storing traditional images as the maps read georeferenced ASCII data files. They have been applied to two sea exercises, in real-time for the full month of August 2018, namely NSF-ALPHA and

POSYDON-POINT and they will be applied in other future exercises. Professor Lermusiaux writes: "In order to successfully coexist with the ocean and optimally utilize and manage marine resources, it is important to monitor and forecast coastal oceans", and these maps *interactively show just that.*

5.2 Future Work

In order to enhance the performance and visualization capabilities of the interactive Leaflet maps, a number of recommendations for future work are listed below.

- **Time and Depth Autoplayers**:
  Presently, the user must manually drag the depth and time sliders to view ocean fields at a different horizontal level or instants of time. A player that automatically portrays the fields in a video format would be a great addition because it gives better insight into pattern changes.

- **Vertical Sections**:
  The present ocean dynamics and uncertainties are all fields at a certain horizontal level (depth). Viewing sections at different lines (parallel to the xy plane) requires a map upgrade into 3D mapping software. A possible venue is using the Cesium JavaScript library.

- **Optimal Path Planning**:
  MSEAS integrates data-driven ocean modeling with the stochastic Dynamically Orthogonal level-set optimization methods to compute and study energy-optimal paths for ocean vehicles [1] [2] [3]. Visualizing these paths on Leaflet maps would comprise another powerful visualization capability.

- **Mobile Application**:
  The present mobile device version of the maps is powerful but it has to be accessed through a browser. Developing a modern application for these interactive maps would be highly attractive.

Bibliography

[1] T. Lolla and P. F. J. Lermusiaux. A forward reachability equation for minimum-time path planning in strong dynamic flows. *SIAM Journal on Control and Optimization*, 2018. Sub-judice.

[2] D. N. Subramani and P. F. J. Lermusiaux. Risk-optimal path planning in uncertain, strong and dynamic flows. *Ocean Dynamics*, 2017. To be submitted.

[3] D. N. Subramani, Q. J. Wei, and P. F. J. Lermusiaux. Stochastic time-optimal path-planning in uncertain, strong, and dynamic flows. *Computer Methods in Applied Mechanics and Engineering*, 333:218–237, 2018.